CSIR - National Institute of Oceanography

Geo-morphological studies and EIA/EMP for the sand mining clusters of Rivers in Goa

Mandovi River

Pre & Post Monsoon

August 2021 Report

Submitted to

Goa State Biodiversity Board (GSBB)
C/o Department of Science, Technology and Environment,
Opp Saligao Seminary, Saligao, Bardez - Goa.
Tel: 0832-2407032 Fax: 0832-2407033

सीएसआईआर – राष्ट्रीयसमुद्रविज्ञानसंस्थान

CSIR-NATIONAL INSTITUTE OF OCEANOGRAPHY

(वैज्ञानिकतथाऔद्योगिकअनुसंधानपरिषद)

(COUNCIL OF SCIENTIFIC & INDUSTRIAL RESEARCH)

दोना पावला, गोवा भारत / DONA PAULA, GOA - 403004 India

फ़ोन/Tel : 91(0)832-2450450

फैक्स /Fax: 91(0)832-2450602

इ-मेल/e-mail : ocean@nio.org

http:// www.nio.org

Executive Summary

This report summarizes the details of field survey undertaken within ~38 km stretches of the Mandovi River. It includes geological and geophysical data acquisition, analysis and important outcomes of the study. As per the project mandate Mandovi River survey have been completed in two phases;

1. **Pre- Monsoon Survey** was carried out from **7th** to **18th March 2020**. Geophysical data, including side scan sonar, single beam echo sounding, and high-resolution seismic, were acquired to study riverbed as well as subsurface characteristics of the Mandovi river. Apart from this, grab sediment samples along 34 stations have also been acquired for geological/geochemical and grain size analysis.

2. **Post- Monsoon survey** was carried out from **2nd** to **4th January 2021**. (26 Line Km side scan sonar, single beam echo sounding, and high-resolution seismic data were acquired to study the post-monsoon geomorphological changes along ~38 km of Mandovi river course.

Key Observations

Sonography survey

- Spatial variations observed in the backscatter sonar intensity and ripple patterns.
- The Side Scan Sonar images of Mandovi river shows varying smooth to rippled to heavily rugged riverbed morphology between off Miramar to Khandepar.
- Point and mid-channel bars are more frequent in upstream region of the river.

Shallow Seismic 2D HR survey

- Sparker system achieved a subsurface penetration of ~3-25 m in the survey area.
- Due to the shallow depth of riverbed, multiples (up to second-order) are observed in the study area.
- Sediment volumes are estimated along selected region using side scan sonar image zonation of sand features and sediment thickness from seismic data.
- Based on EIA/EMP studies eight feasible sand mining regions are identified.

Sediment Sampling

- Sediment samples were collected at different stations using a small hand grab sampler.
- Sand is the most dominates sediment size followed by silt.

Contents

List of Figures

List of Tables

Chapter 1. Introduction

Background

Undoubtedly sand is essential part of river ecosystem. Like flow and fish, it helps rivers stay healthy, sand is critical for ground water recharge, replenishes the nutrients in moving water and provides habitat to numerous forms of aquatic and riparian fauna. Sand has become an essential component of most of modern infrastructure. From roads to buildings and other structure, usage of sand is ubiquitous all over the planet. Sand mining is the extraction of sand from beaches or ocean and riverbeds. The dredging and mining often cause several alterations to the physical characteristics of both a river and riverbed. The erosion caused by the process of mining to the ocean or river floor can also adversely affect the biodiversity of the region (river and riparian habitats). Although several policy measures have been undertaken, the sheer demand for sand worldwide has given rise to a large network of sand mining operators including Goa, India.

To address impact of sand mining on the health of the riverine systems of Goa, four major rivers have been identified viz; ***Chapora, Terekhol, Mandovi*** and ***Zuari*** rivers. In each of these rivers a total of twenty-four active sand mining clusters have been identified (Annexure-I). Other than the above four, Goa harbors few more rivers. This proposal also includes an estimate for carrying out studies in the nine rivers (***Sal, Talpona, Galjibag, Cumbarjua, Valvanti, Mapusa, Sinquerim, Khandepar, Kushavati***) and at other sand mining areas in other rivers as second phase of this project. Presently there is no data available for the rivers with respect to sand, availability, areas, its extraction etc. Goa State Biodiversity Board (GSBB) an autonomous body of Government of Goa under Department of Science, Technology and Environment, would like to carry out a study to understand the geo-morphology, bathymetry, sand budgetary and flow dynamics of these clusters and the impact of sand mining on the biodiversity of these identified river clusters in in Goa. GSBB has approached CSIR-National Institute of Oceanography (CSIR-NIO), since the CSIR-NIO is having scientific expertise, infrastructural and logistic facilities and capability for carrying out such studies.

"In the present report the study is focused on the river Mandovi for Geo-morphological studies and EIA/EMP for the sand mining clusters (Fig. 1)."

Chapter 2*. *Data Acquisition: provides the detail information about the geophysical survey and various equipment's deployed for the survey like side scan sonar (SSS) for imaging the geomorphology of the river bed, single beam echo sounding for imaging the river bed depth, high resolution seismic (HRS, squid) system for imaging the subsurface structures below the river bed.

Chapter 3*. *Data Processing: provides the detail information about the geophysical data processing and various parameters for processing the side scan sonar (SSS), single beam echo sound, high resolution seismic (HRS). Geological sampling location are determined from geophysical survey samples were collected for geological studies.

Chapter 4**. **Interpretation: provides the detail interpretation and cross correlation between different geophysical data sets across the Mandovi river for identification of various geomorphological features associated with the sand distribution (sand ripple marks, sand bars), river bank, active mining, exposed bed rock and river bank erosion~~,~~ from side scan sonar data, corresponding depth from single beam and subsurface sediment thickness from high-resolution seismic data.

Chapter 5**. **Geological observations: provides the detail analysis and observations from the geological samples collected across the river Mandovi.

Chapter 6. Post Monsoon Geophysical Survey: provides the comparative studies of Mandovi river based on Geophysical data.

Chapter 7. Conclusion: provides the results like sand volume and weight, grain size, microscopic imaging based on pre and post monsoon geophysical and geological sampling.

Chapter 2. Data Acquisition

Geophysical data acquisition

Mandovi River is one of the main rivers of Goa, India. It enters from the high lands of Western Ghat in Uttara Kannada district of Karnataka to table lands via Satari taluka of Goa. Before debouching near Aguada headland (Goa) in western Arabian sea, it covers ~45 km. It runs north-westward from Khandepar and finally changes its course to south-westward at Piligaon.

General

Geophysical survey is a systematic collection of multi-platform geophysical data for spatial studies. They have many applications in geology, archaeology, mineral and energy exploration, oceanography, and engineering. Geophysical surveys are used in industry as well as for academic research. Such surveys are classified as seismic and non-seismic and provide various levels of detail, but all generate useful data based on the purposes for which the surveys are conducted. In the present study, the geophysical surveys carried out include seismic, and sonography survey along with the single beam bathymetry for the Mandovi river (Fig.1).

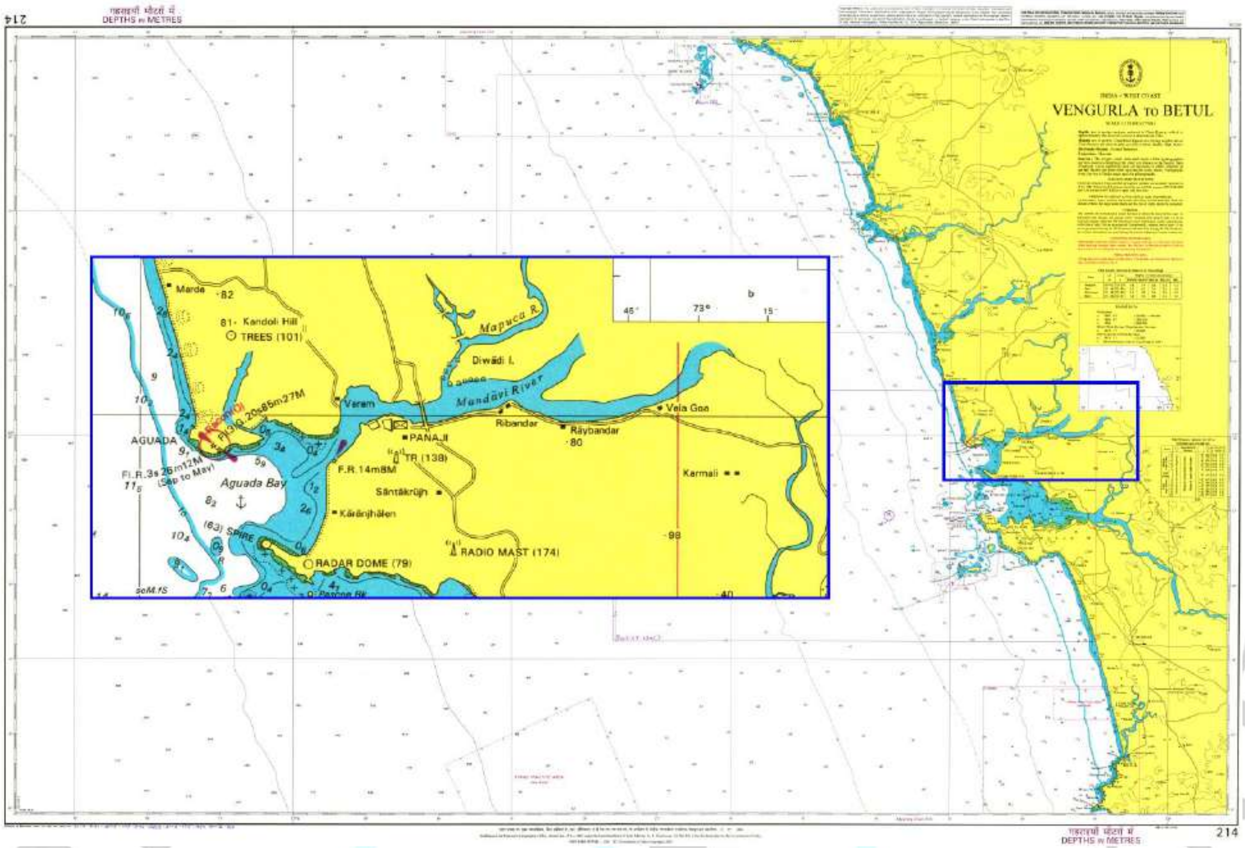

Figure 1. Hydrographic Map of Goa. Insight zoom area of river Mandovi.

Geodesy and controls

The survey was conducted in WGS 84 datum i.e. World Geodetic System version 84 spheroid which is invariably used by the various constellation of Global Navigation Satellite System (GNSS).

GEODETIC PARAMETERS	
Satellite Datum	
Spheroid	WGS-84
Datum	WGS 84
Semi-Major Axis	6378137.000 m
Semi Minor Axis	6356752.314 m
Inverse Flattening	298.2572
Projection Parameters	
Grid Projection	Universal Transverse Mercator
Latitude of Origin of Projection	0□ (Equator)
Longitude of Origin of Projection	75° E, Zone 43
Hemisphere	North
False Easting (meters)	500000
False Northing (meters)	0
Scale Factor on CM	0.9996
Units	Meters

Table 1. Geodetic survey parameters

Survey Plan

The entire geophysical survey was planned in two phases. Phase – I consisting of side scan survey (SSS), single beam echosounder profiling and seismic sparker survey were carried out along the navigating channel of the Mandovi river. In a similar manner, Phase-II consisting of sediment sample was carried out using a hand-held grab sampling equipment (Google map; Fig.2).

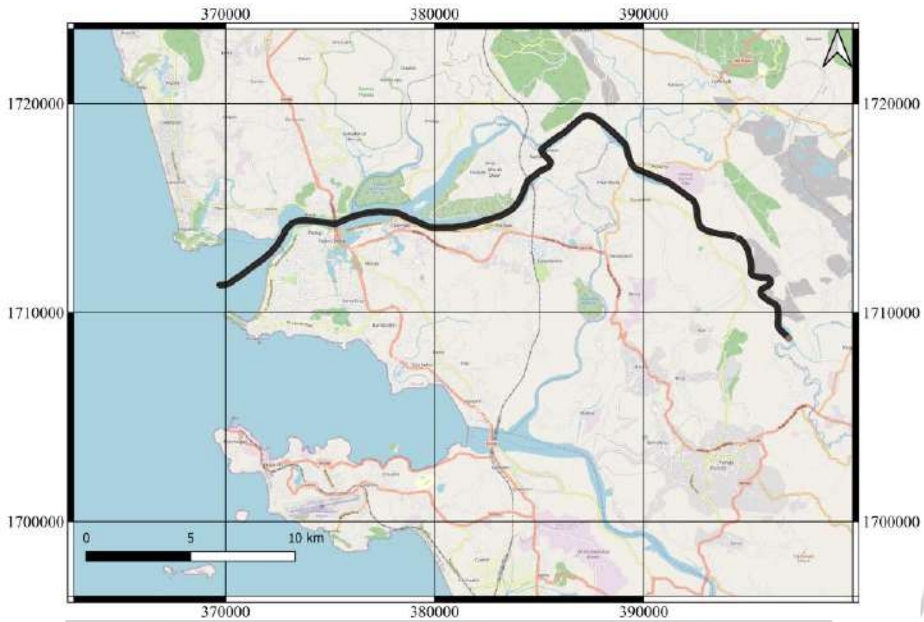

Figure 2. Google Map of the survey region (Mandovi River)

Survey boats deployed for geophysical survey in Mandovi river

Two different boats were deployed for various geophysical survey in the Mandovi river for side scan sonar (SSS), single beam echosounder profiling, and high resolution seismic (HRS) survey (Fig.3).

Figure 3. Boat deployed for survey for side scan sonar (SSS) imaging, single beam echosounder profiling, high resolution seismic (HRS squid) survey and geological sampling across the Mandovi river.

Single Beam Echo sounder profiling

Data Acquisition Software

The acquisition software used is HYPACK® Max (Fig. 4a), a marine surveying, positioning, and navigation software package. The software provides interface between various sensors such as motion sensor, heave sensor, global positioning system, echosounder, seismic data acquisition and side-scan sonar. The acquisition hardware is composed of three separate units: a GPS system on the survey vessel (rover), a motion sensor (vessel heave, pitch, and roll), and a Single beam echosounder. All the above hardware units were interfaced with acquisition system (HYPACK® Max). The acquisition software combines the data streams from the various components into a single raw data file, with each device string referenced by a device identification code and timestamped to the nearest millisecond.

The HYPACK® acquisition software combines the data streams from the various components into a single raw data file, with each device string referenced by a device identification code and timestamped to the nearest millisecond. The raw data thus gets recorded on hard disk of the computer, which were copied to the portable hard disc. The time stamping to navigation and other geophysical data was accomplished in Greenwich Mean Time (GMT) provided by the Global Positioning System (GPS) receiver clock throughout the survey.

Navigation and Planning

The survey track lines were planned, oriented, in the navigation channel with the help of local navigator as no depth values are readily available in such a way that the underway survey would fulfil the objectives of the project indicated in the WORK. The survey vessel is navigated and maneuvered along navigation track lines by the master of the survey boat. In order to assist the master in track navigation, a helmsman monitor was placed in the wheel house of the vessel. This was interfaced to the data acquisition PC, running one of the most widely used software package called HYPACK® Max. It is basically a Windows PC based integrated software package for automated hydrographic data acquisition and processing routines, developed by Xylem Inc., USA.

The data from the GPS receiver, motion sensor, and echosounder are streamed in real time to a computer running the Windows operating system. Over to this, it also provides tools to i) Design preplanned survey track lines ii) Navigate along the planned track lines iii) Provide position data to other geophysical systems (echo sounder and high-resolution sub-bottom profiler) iv) Log raw position and depth data and v) Realize the quality control in real time navigation.

Bathymetric Equipment and Software's

The single beam bathymetric survey equipment consists of boat-based hull mounted Bathy-500HD echosounder. The Bathy-500HD is a high-resolution, precision echo sounder. It is basically a triple frequency echosounder having 33 kHz, 50 kHz and 210 kHz frequency acoustic bursts (Fig. 4a, b). It is designed exclusively for hydrographic marine surveys up to 100 meters of water depth. It meets or exceeds all current IHO hydrographic requirements for single beam echo sounders.

The Bathy-500HD system is configured as a flexible acoustic measurement sensor device capable of providing an excellent solution for shallow water hydrographic applications. Both applications make use of the appropriate signal processing features to perform accurate and reliable bottom digitizing. The Bathy-500HD makes use of sophisticated algorithms for first/peak bottom echo detection, automatic mode controls for: receiver gain, bottom tracking, pulse length and power level controls greatly reduce the probability of inaccurate bottom detection/tracking.

Bathymetric surveys allow us to measure the depth of a river bed as well as map the underwater features on the seabed. Bathymetric charts are typically produced to support safety of surface navigation, and usually show sea-floor relief or terrain as contour lines and selected depths soundings.

Sparker data acquisition system

High-resolution shallow seismic system (make: Applied Acoustics Squid 500) was deployed to acquire the sub-bottom information of the region. The system includes Power Supply, Trigger capacitor bank, (Fig. 4c), hydrophone streamer array and an acquisition unit (model Mini-Trace II). In this technique, a source of seismic energy (squid system) is towed behind the survey vessel just below the sea surface. The transmitted pulse travels through the water column and sub-surface and are reflected when changes in acoustic impedance are encountered. Acoustic impedance changes commonly occur at the boundaries; i.e., interfaces between water and sediments, inter-sediments, and sediments and basement.

The reflected pulses travel back towards the sea surface, and the reflections are detected by an 8-element hydrophone. These reflections are converted to an electrical signal, which is amplified and converted to digital samples and stored in the hard disk of the data acquisition system (Mini Trace II) in native GeoTrace format. This data is then processed, filtered and displayed in graphic form as a function of travel time. The raw data is copied in SEGY format and later processed at CSIR-NIO using seismic data processing software ProMAX.

Side scan sonar

EdgeTech 4125 digital side scan sonar digital geophysical data acquisition system was used for SSS data on board (Fig. 4d)

Rub Test: The side-scan sonar system was set up on the deck of the respective survey vessels and a ‘rub test’ was carried out on both port and starboard transducers of the tow fish.

Wet Test: The tow fish was thereafter, lowered into the water and a ‘wet test’ was performed to check that echo from targets were returning to both the channels. The gain and grey-scale settings were adjusted to balance the port and starboard channels of the side-scan sonar system.

Side-scan sonar data was acquired using SonarWiz software geophysical digital data acquisition system.

The raw data was recorded in *.jsf and *.xtf format and the xtf format is used for processing the data. The EdgeTech acquisition software displayed the real time acoustic data on the computer screen for online quality control (QC). Output was controlled by specifying or editing various parameters, e.g., filter settings, automatic bottom tracking settings for known fish height at any time, time variable gain settings, output file format (XTF) settings. SonarWiz data processing software package was finally used to process the acquired side scan sonar data.

Dual-channel dual frequency EdgeTech 4125 side-scan sonar performed well during the survey. The tow system was operated using recommended manufacturers procedures. The tow fish was towed astern of the survey vessel over an arm.

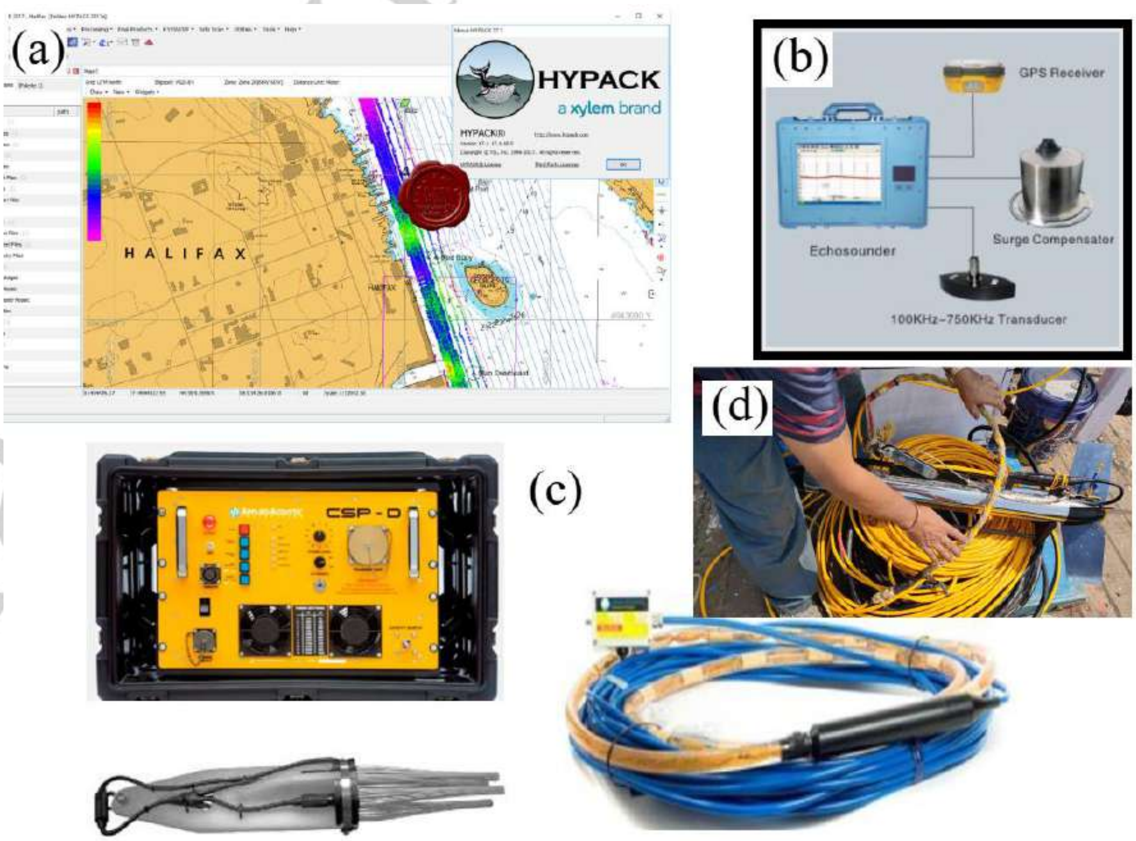

Figure 4.a) Hypack software used for recording Navigation and single beam echosounding data; b) Single beam echosounding system; c) Squid Sparkar System with 8 element streamer; d) Side Scan Sonar system (400kHz/900kHz).

Sediment Sampling

In Phase-II, we carried out sediment sampling at selected locations based on the side scan sonar images across the Mandovi river region (Fig. 5). The sediment samples are collected for geological analysis and cross correlated with the surface features interpreted from side scan sonar (SSS) to understand river bed morphology.

Figure 5. Sediment sample (hand-held grab sampler) photographs in the Mandovi river.

Chapter 3. Data Processing

Geophysical data processing

High resolution Seismic data processing

The raw seismic data collected across the Mandovi river for subsurface imaging is processed for increasing the signal to noise ratio for better subsurface imaging. Raw data was loaded with Seismic Unix processing software and bandpass filtering (400-450-1900-2000) was applied. We observed riverbed multiples up to 3rd order.

Single beam bathymetry data processing

Raw single beam echosounder bathymetry data collected along the navigation track line for real-time monitoring the depth of the riverbed.

Side Scan Sonar Data Processing

Raw data processing and analysis is carried out through “SonarWiz5” software following processing steps listed in Fig. 6. Common processing steps include bottom tracking, signal processing (automatic gain control, beam angle correction, time varying gain), and offset & layback correction for determining towed sensor positions. The resultant side scan sonar image is created by mosaicking which is a process of assembling geo-referenced sonar images from adjacent track lines to create a comprehensive image of the seabed that represents the acoustic character of the seabed of the survey area. Finally, processed data and images are exported into formats compatible with Geographical Information Systems/other spatial image analysis software.

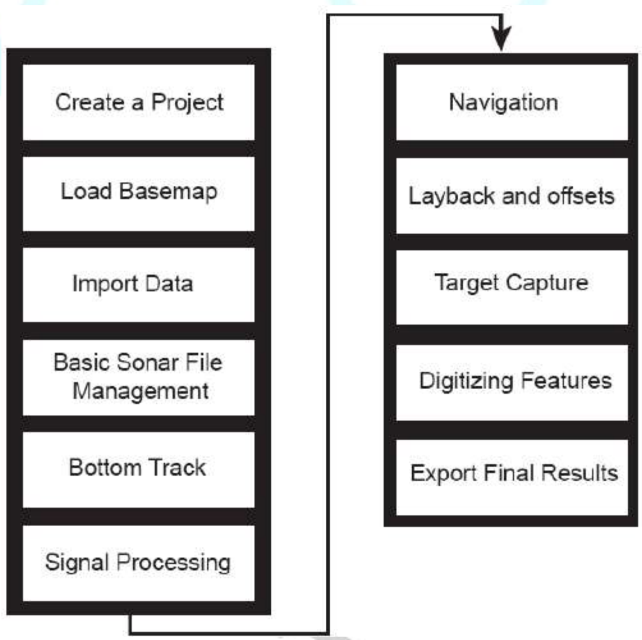

Figure 6. Flow diagram of side scan sonar data processing system.

Side Scan Sonar Data

The side scan sonar (SSS) is deployed from the starboard side ~ 0.5 m below water column and towed. The survey is navigated along the channel at ~3.5 knots speed and the continuous data is collected from mouth of the Mandovi River (Off Miramar) to Khandepar (Fig. 2). The side scan sonar data have been recorded with 100 m swath range in both (i.e., star and port) side of the boat, which provided a total coverage of 200 m (Highlighted in yellow rectangle box; Fig. 2). The side scan sonar image is the intensity image of the backscatter from the riverbed and river banks.

Fig. 7 shows side scan sonar images of various salient features from different locations within the river basin. Fig.7a shows river banks and rock debris at bank and mining signatures on the riverbed. Fig.7b side scan sonar image overlaid on the google map highlights roads at the river banks rock outcrops and rock debris along with bridge pillar base and its shadow. Fig.7c highlights confluence points of a tributary which joins the main stream and some mining signatures. Fig.7d shows some more examples of mining in the Mandovi river.

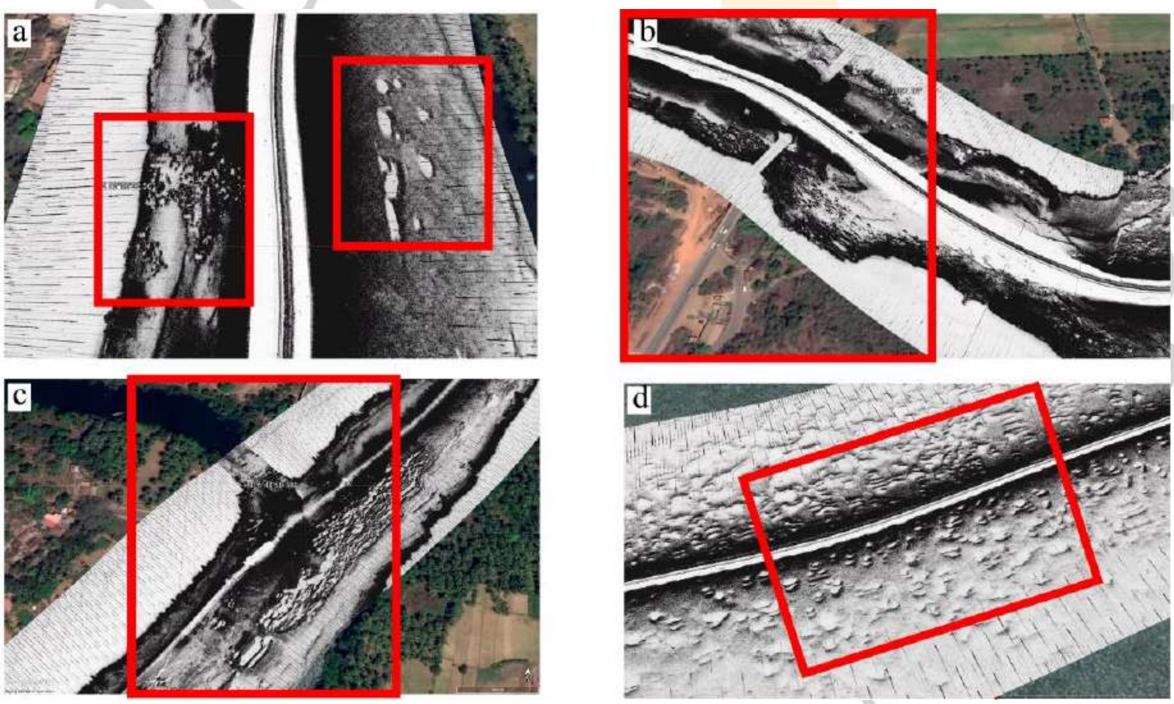

Figure 7. Side Scan Sonar images. A) River banks and small boulders, active mining, b) shadow zones of bridge pillars c) confluence of river channel d) active mining marks.

Chapter 4. Interpretation

Major features identified from the side scan sonar (SSS) imaging

Riverbed morphology through the side scan sonar images have been carefully analyzed in order to study the geomorphology of the river, and to map mining zones in the study area. The processed images are presented along with a key map in Figures 17 to 28. The analysis of the side scan sonar images reveals that the riverbed is carpeted by sediments in the entire surveyed area except at few locations. Rock outcrops in the riverbed are observed near Narve, Candola, and Navelim. Apart from this, river bank rock outcrops and rock debris are also identified in up-stream Volvoi (Figs. 8-9).

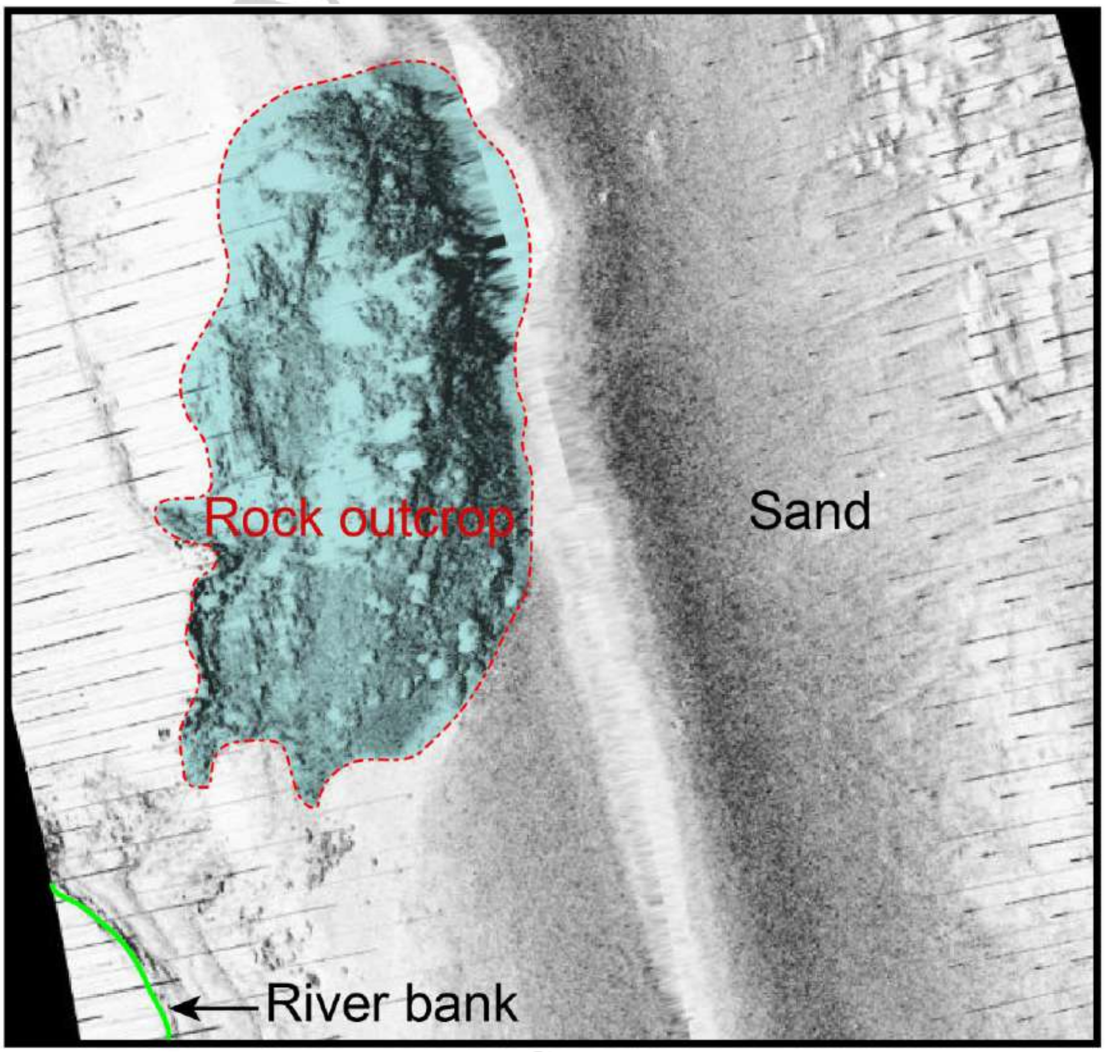

Figure 8. Sonogram showing rock outcrop at Candola, near Amona bridge.

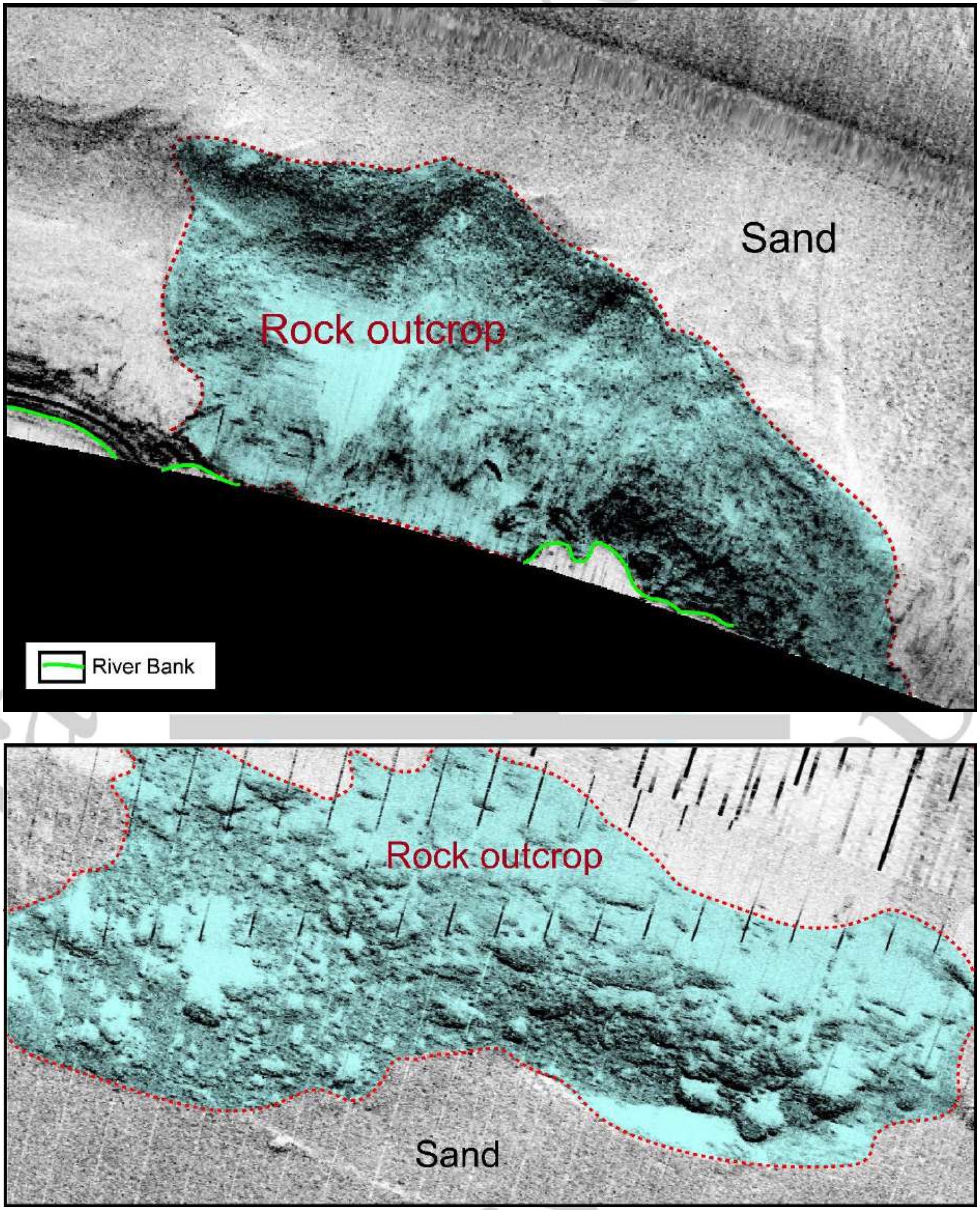

Figure 9. Sonogram showing rock outcrop and debris near the river bank.

.

Based on morphological features such as ripple marks and sand bar along with tonal and textural variation in the backscatter data, sand deposits on the riverbed are identified as shown in Fig. 10. Sand boundaries in each sonogram have been delineated and some select locations are presented in Figures 17-28.

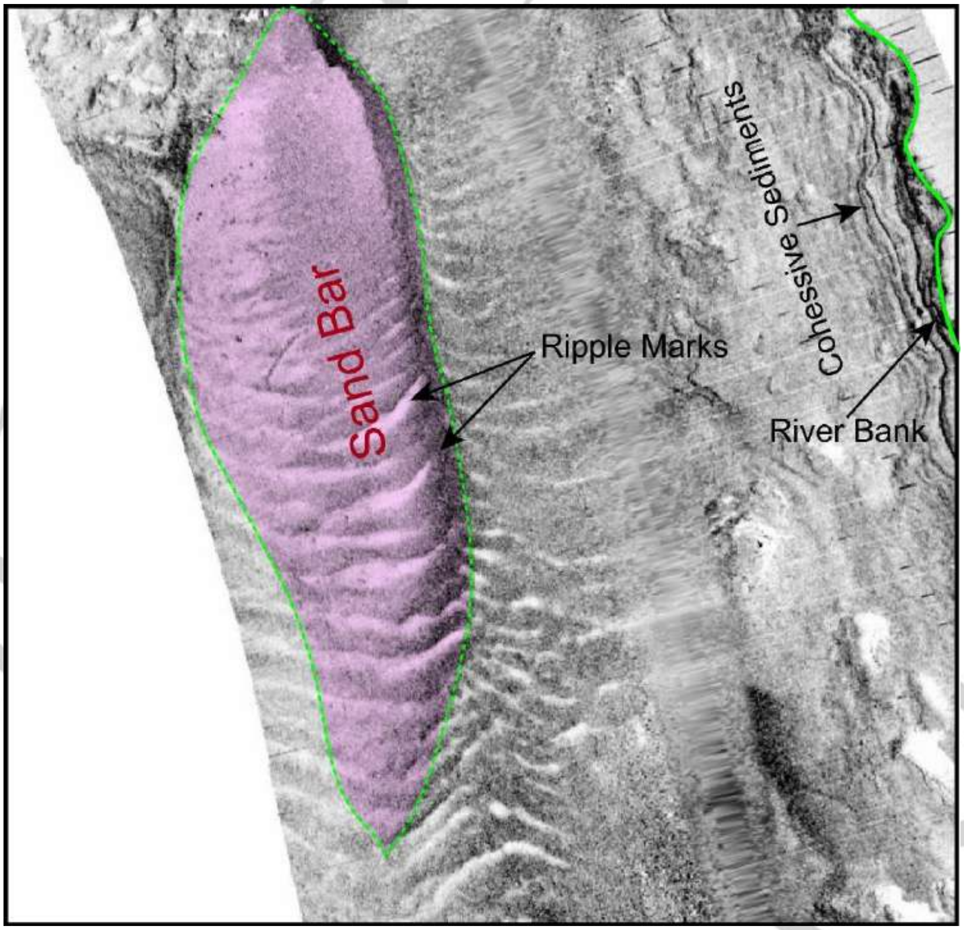

Figure 10. Sonogram showing sand bar and ripple marks.

At certain locations, side scan sonar images show zones with signatures of sediment excavation. These zones are interpreted as mining zones. Based on the appearances of excavation marks, these active mining zones can be categorized in two types: type-1 mining zones show elongated excavation marks and one such mark is shown in Fig.11.

Type-2 mining zones show rounded to elliptical excavation marks and a representative example of ~20-25 m diameter is shown in Fig. 12. Two different types of excavation marks signify variation in mining practice. Type-1 mining is predominant in Carambolim-Narora, Golwada-Narve, Piligao-Candola, Amona, Navelim regions of the river basin, whereas Type-2 mining zones are located in Navelim-Volvoi, and Sateri-Khandepar region.

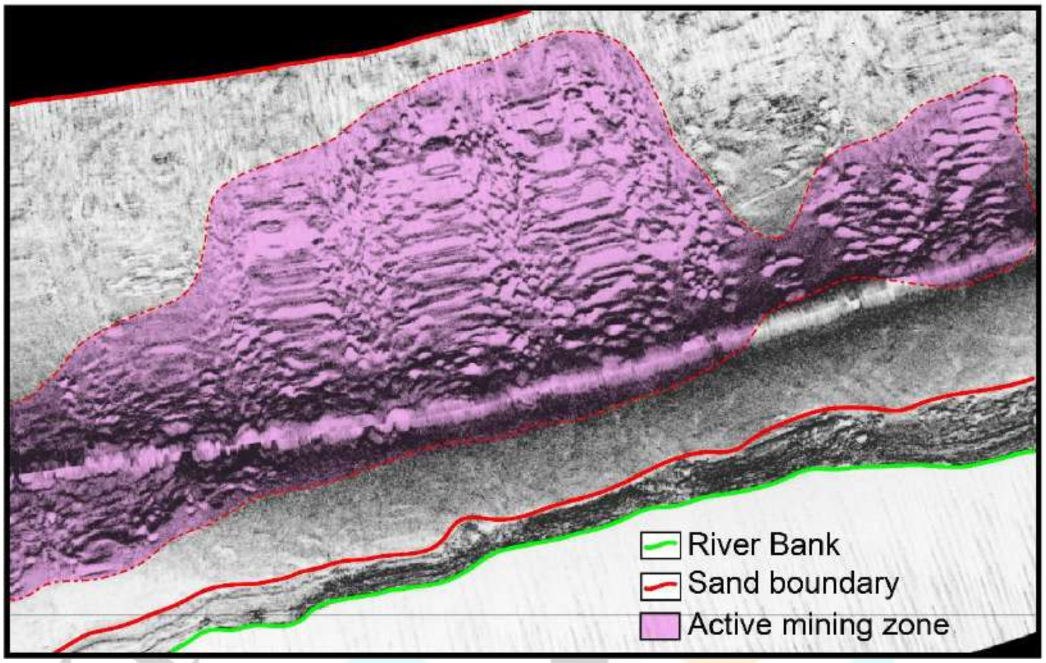

Figure 11. Sonogram showing type-1 mining zone at Navelim-Betqui

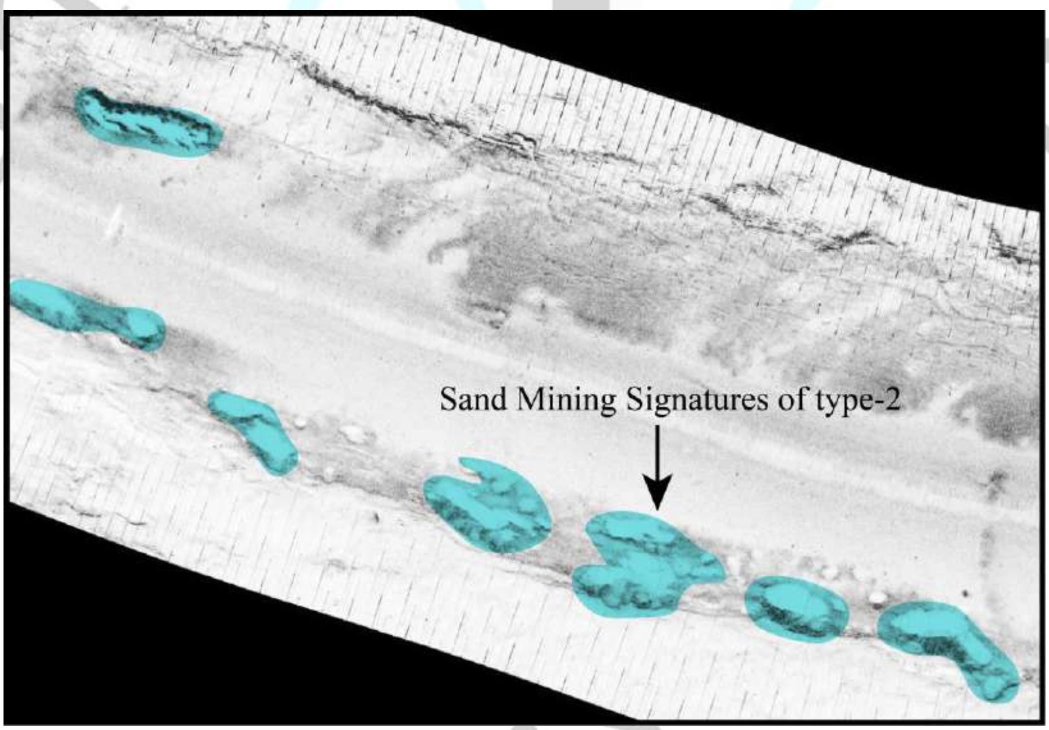

Figure 12. Sonogram showing type-2 sand mining zone in Navelim-Volvoi region.

Color legends in Geophysical interpretation

Integrated geophysical plot highlighting the geomorphology based on side scan sonar (SSS) imaging, real time river bed bathymetry using single beam echo sounding and subsurface sediment structures derived from high-resolution sparker seismic data (Figures 14 to 20). The side scan sonar (SSS) image is referenced with WGS84 Universal Transverse Mercator (UTM) coordinate system and also in relative distance mode. Hereafter, the top X-axis is UTM-X, right Y-axis is UTM-Y and bottom and left axis show relative distance in m. The side scan sonar profile in Figures 14a-20a is interpreted with confirmed sand boundaries (red solid line), unconfirmed sand boundary (dotted red), outcrop (cyan), river bank (green), active mining region (pink solid), geological sample locations (green star) and the HRS seismic track is highlighted in solid blue line with the trace no. The bridges across the river are shown with Yellow and interpreted sand bars as solid black lines. Figures 14b-20b represent real-time single beam echo sounder data (Solid blue) providing the river bed depth profile along survey line. Figures 14c-20c show interpreted riverbed (green) and acoustic basement (red) usually a bedrock, which are used for the calculation of sediment thickness.

The seismic data is acquired in time domain and is converted to depth by using a constant velocity of 1500 m/s. The sediment volumes are calculated as follows: difference between the bedrock and riverbed provides the sediment thickness along the seismic track. We assume that the sediment thickness goes to zero at the boundary of the sand zone. Assuming a linear sediment thickness between the seismic track line and boundary of sand zone, the cross section is calculated from the area of triangle as shown in Figure 13. The volume is calculated by multiplying the cross-section area with the incremental distance along the survey line.

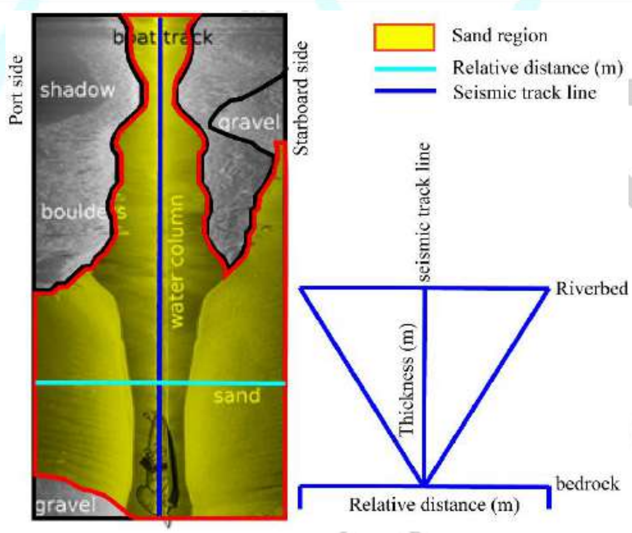

Figure 13. Schematic representing the calculation of sediment resource along the river profile

The total weight of sediment in tonnage is calculated by multiplying the volume with the bulk density of sediment of 1.6 g/cm^3 (equivalent to 1.6 Tonnes/m^3).

Narve

The SSS image across **Narve village** region covers an area of (200x2200) m^2 from the center of the navigation (blue track line). It shows probable sand boundary (red), mining zones (pink) and a rock outcrop (cyan) along with river bank (green) (Fig. 14a). Single beam bathymetry data shows the real-time depth, which varies between ~7.8 and 16.2 m (Fig. 14b). One geological sample location (**station 78**) is within the span of side scan sonar image (Fig.14a). The details of sediment sample analysis are provided in Table 3. The seismic data, interpreted in both time and depth domain, shows the riverbed depth varies between ~7.5 and 16 m (green). The interpreted bedrock is observed in the seismic data around depth of ~8.5 to 17 m (red) (Fig.14c). The estimated sediment volume is **655737 m^3** equivalent to **1049180 tons** of sediments predominately of sand grain size.

Piligao

The SSS image across **Piligao** covers an area of (200x2200) m^2 from the center of the navigation (blue track line). It shows probable sand boundary (red), mining zones (pink) and a rock outcrop (cyan) along with river bank (green) on one side (Fig.15a). Single beam bathymetry data shows the real-time depth, which varies between ~6.2 and 13.9 m (Fig. 15b). One geological sample location (**station 80**) is within the span of side scan sonar image. The details of sediment sample analysis are provided in Table 3. The seismic data, interpreted in both time and depth domain, shows the riverbed depth varies between ~7.4 and 14.2 m (green) and interpreted bedrock (red) around ~21 m (Fig. 15c). The estimated sediment volume is **~1042480 m^3** equivalent to **~1667968 Tons** of sediments predominately of sand grain size.

Across Amona Bridge

The SSS image across **Amona Bridge** covers an area of (200x2200) m^2 from the center of the navigation (blue track line). It shows probable sand boundary (red), mining zones (pink) and a rock outcrop (cyan) along with river bank (green) (Fig. 16a). Single beam bathymetry data shows the real-time depth, which varies between ~6.5 and 16.5 m. Two depressions are identified from the single beam bathymetry (Fig.16b) and seismic data (Fig.16c), where the depth of riverbed increases from 9 m to 16.5 m. One geological sample location (**station 83**) is within the span of side scan sonar image (Fig. 16a). The details of sediment sample analysis are provided in Table 3. The seismic data, interpreted in both time and depth domain, shows the riverbed depth varies between ~7.7 and 16 m (green) and bedrock (red) between ~11 and 22 m (Fig. 16c). The estimated sediment volume is ~**855419 m^3** equivalent to **~1368670 Tons** of sediments predominately of sand grain size.

Vedanta Pig Iron Plant, Navelim

The SSS data across the **Vedanta Pig Iron Plant** covers an area of (200x2100) m^2 area from the center of the navigation (blue track line). It shows probable sand boundary (red), mining zones (pink) and a rock outcrop (cyan) along with river bank (green) (Fig.17a). Single beam bathymetry data (Fig.17b) shows real-time river bed depth varying between ~7.8 and 14.5 m. One geological sample location (**stations 87**) is within the span of side scan sonar image (Fig.17a). The details of sediment sample analysis are provided in Table 3. The seismic data, interpreted in both time and depth domain, shows the riverbed depth varies between ~7.6 and 14.8m (green) and bedrock (red) depths between ~9.5 and 20.5 m (Fig. 17c). The estimated sediment volume is **~631923 m^3** equivalent to **~1011078 Tons** of sediments predominately of sand grain size.

Navelim-Volvoi

The SSS image across the **Navelim-Volvoi** covers an area of (200x2200) m^2 area from the center of the navigation (blue track line). It shows probable sand boundary (red), mining zones (pink) and a rock outcrop (cyan) along with river bank (green) (Fig.18a). Single beam bathymetry data (Fig.18b) shows real-time river bed depth varying between ~9.9 and 16.5 m. One geological sample location (**stations 99**) is within the span of side scan sonar image (Fig.18a). The details of sediment sample analysis are provided in Table 3. The seismic data, interpreted in both time and depth domain, shows the riverbed depth varies between ~9.5 and 16.0 m (green) and bedrock (red) depths between ~14.9 and 19 m (Fig.18c). The estimated sediment volume is **~443788 m^3** equivalent to **~710061 Tons** of sediments predominately of sand grain size.

Volvoi-Cotombi

The SSS image across **Volvoi-Cotombi region** covers an area of (200x2000) m^2 m area from the center of the navigation (blue track line). It shows probable sand boundary (red), mining zones (pink) and a rock outcrop (cyan) along with river bank (green) (Fig. 19a). Single beam bathymetry data shows real-time river bed depth varying between ~3.8 and16.6 m. A deep valley like feature is identified from the single beam bathymetry (Fig. 19b) and seismic data (Fig.19c). One geological sample location (**stations 96**) is within the span of side scan sonar image (Fig.19a). The details of sediment sample analysis are provided in Table 3. The seismic data, interpreted in both time and depth domain, shows the riverbed depth varies between ~3.8 and 16.5 m (green) and bedrock (red) depths between ~3.7 and 18.75 m (Fig.19c). The estimated sediment volume is **~372501 m^3** equivalent to **~596002 Tons** of sediments predominately of sand grain size.

Khandepar

The SSS image across Khandepar region covers an area of (200x2200) m^2 area from the center of the navigation (blue track line). It shows probable sand boundary (red), mining zones (pink) and a rock outcrop (cyan) along with river bank (green) (Fig. 20a). Single beam bathymetry data shows real-time river bed depth varying between ~3.9 and 14.5 m. Three deep depressions are identified from the single beam bathymetry (Fig. 20b) and seismic data (Fig. 20c). One geological sample location (**station 92**) is within the span of side scan sonar image (Fig.20a). The details of sediment sample analysis are provided in Table 3. The seismic data, interpreted in both time and depth domain, shows the riverbed depth varies between ~3.8 and 14.9 m (green) and bedrock (red) depths between ~4 and 15 m (Fig. 20c). The estimated sediment volume is **~151039 m^3** equivalent to **~241662 Tons** of sediments predominately of sand grain size.

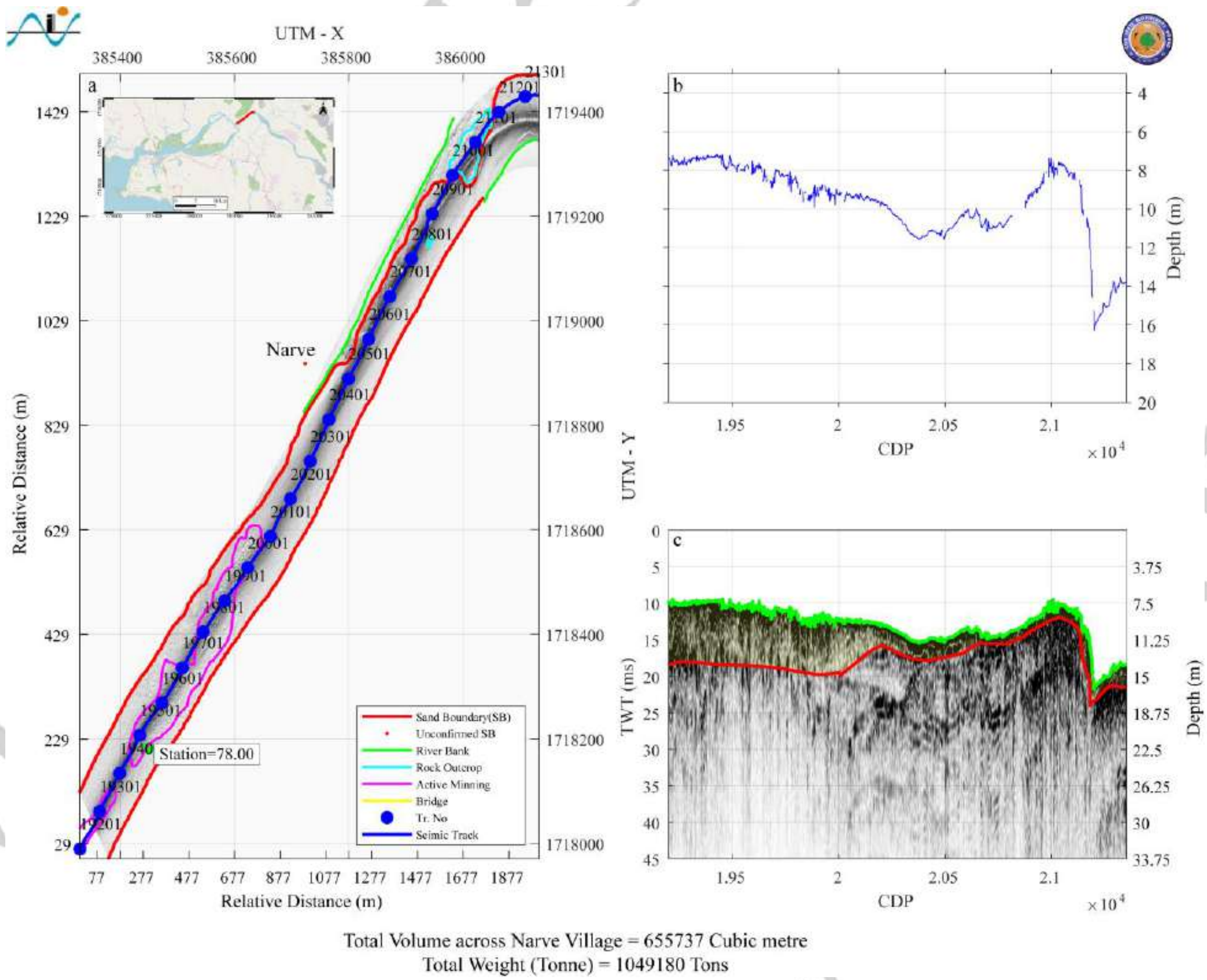

Figure 14. Geophysical data across Narve village. (a) Side scan sonar (SSS) image (b) single beam echosounder bathymetry. (c) high resolution seismic data

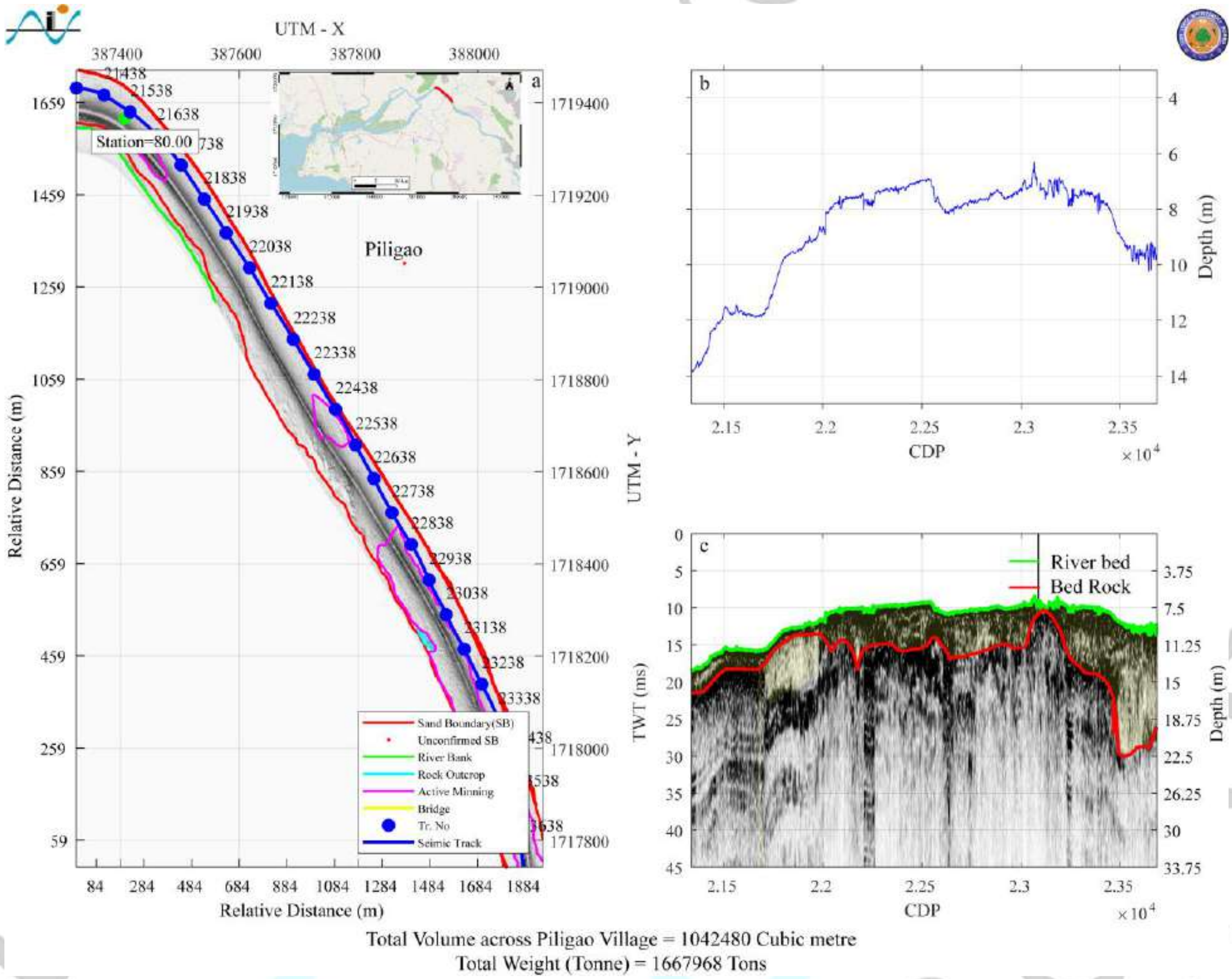

Figure 15. Piligao geophysical data. (a) Side scan sonar (SSS) image (b) single beam echo-sounder bathymetry. (c) high resolution seismic data

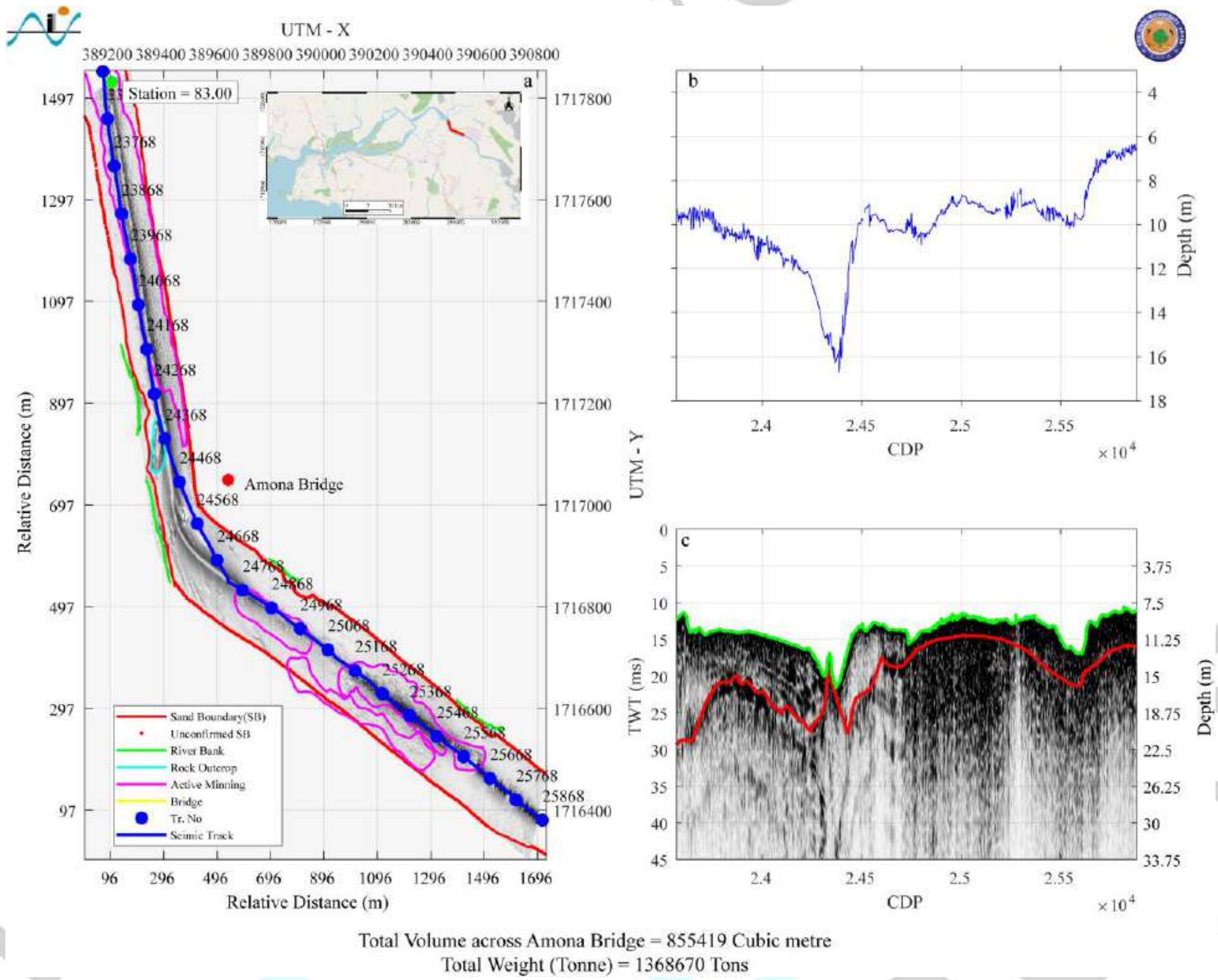

Figure 16. Geophysical data across Amona bridge. (a) Side scan sonar (SSS) image (b) single beam echosounder bathymetry. (c) high resolution seismic data

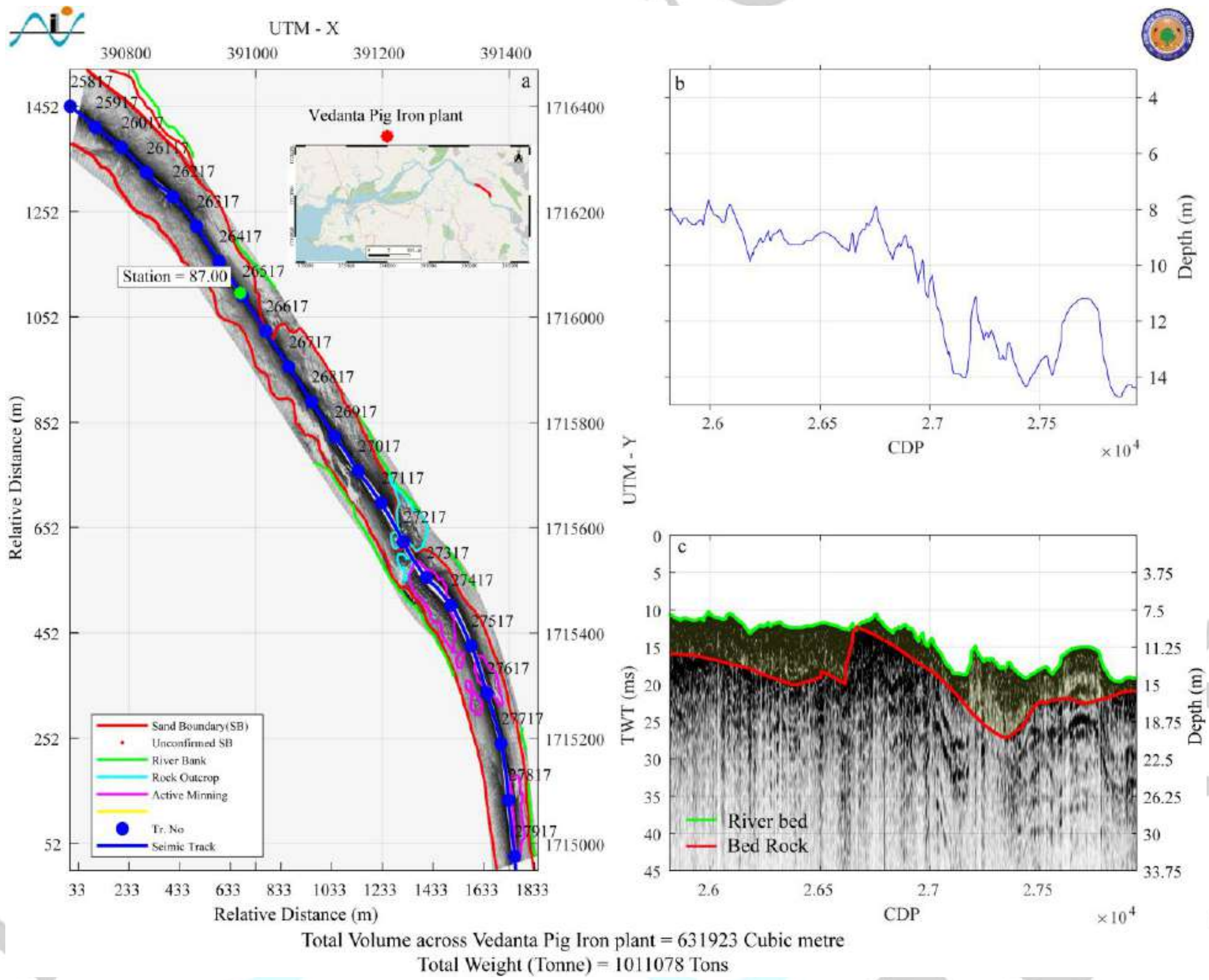

Figure 17. Geophysical data near Vedanta Pig Iron plant, Navelim. (a) Side scan sonar (SSS) image (b) single beam echosounder bathymetry. (c) high resolution seismic data

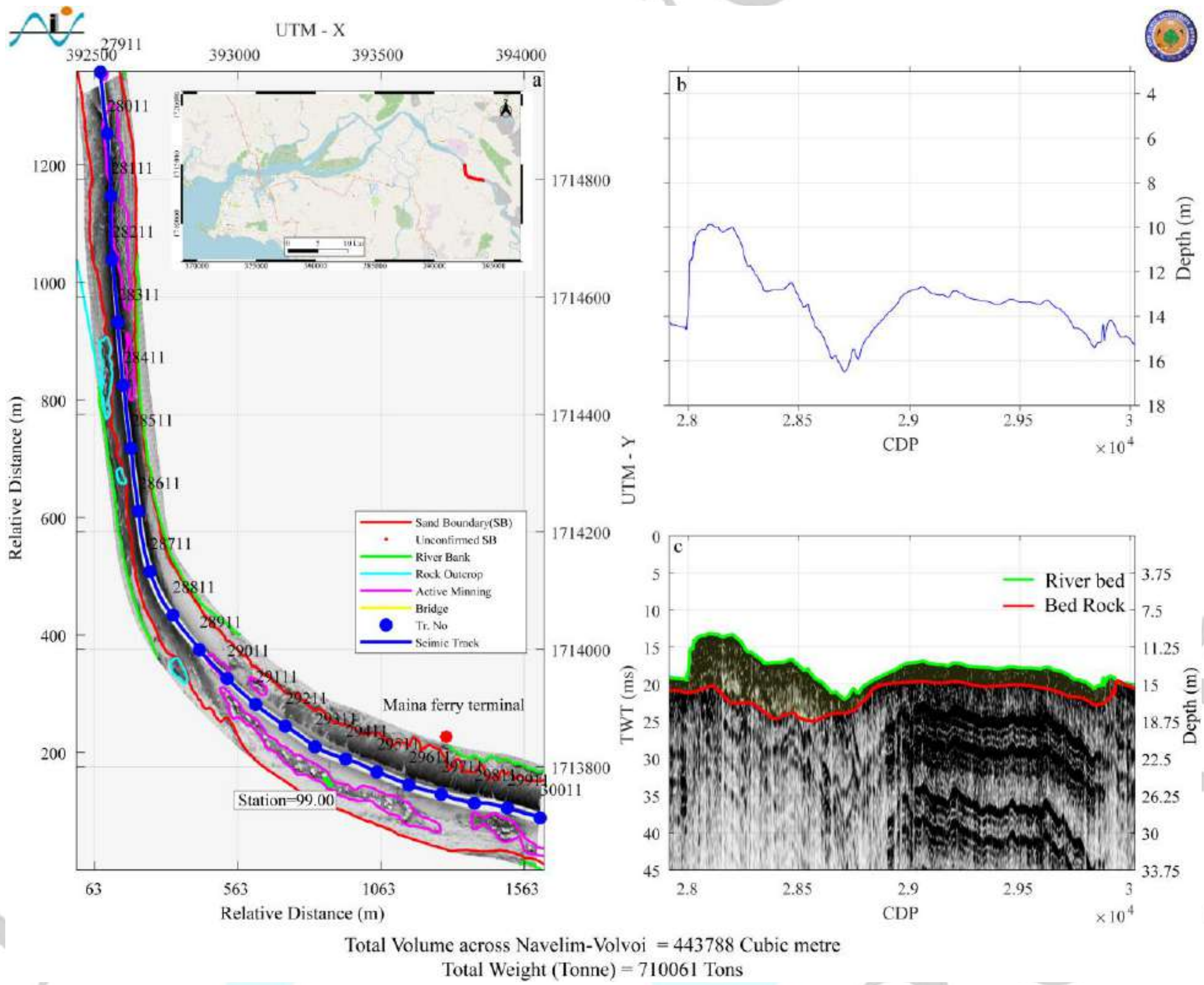

Figure 18. Geophysical data across Navelim-Volvoi. (a) Side scan sonar (SSS) image (b) single beam echosounder bathymetry. (c) high resolution seismic data

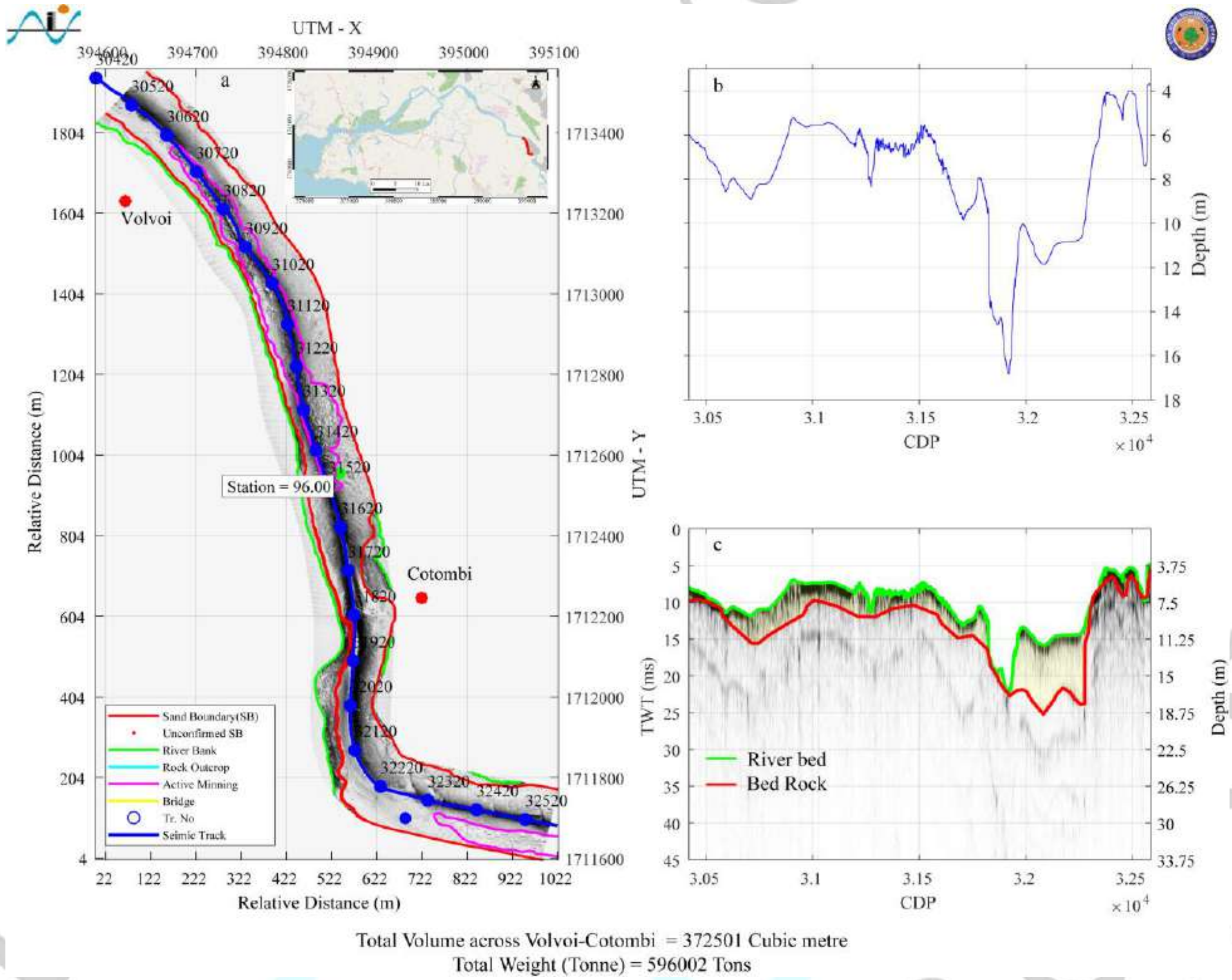

Figure 19. Geophysical data across Volvoi-Cotombi. (a) Side scan sonar (SSS) image (b) single beam echosounder bathymetry. (c) high resolution seismic data

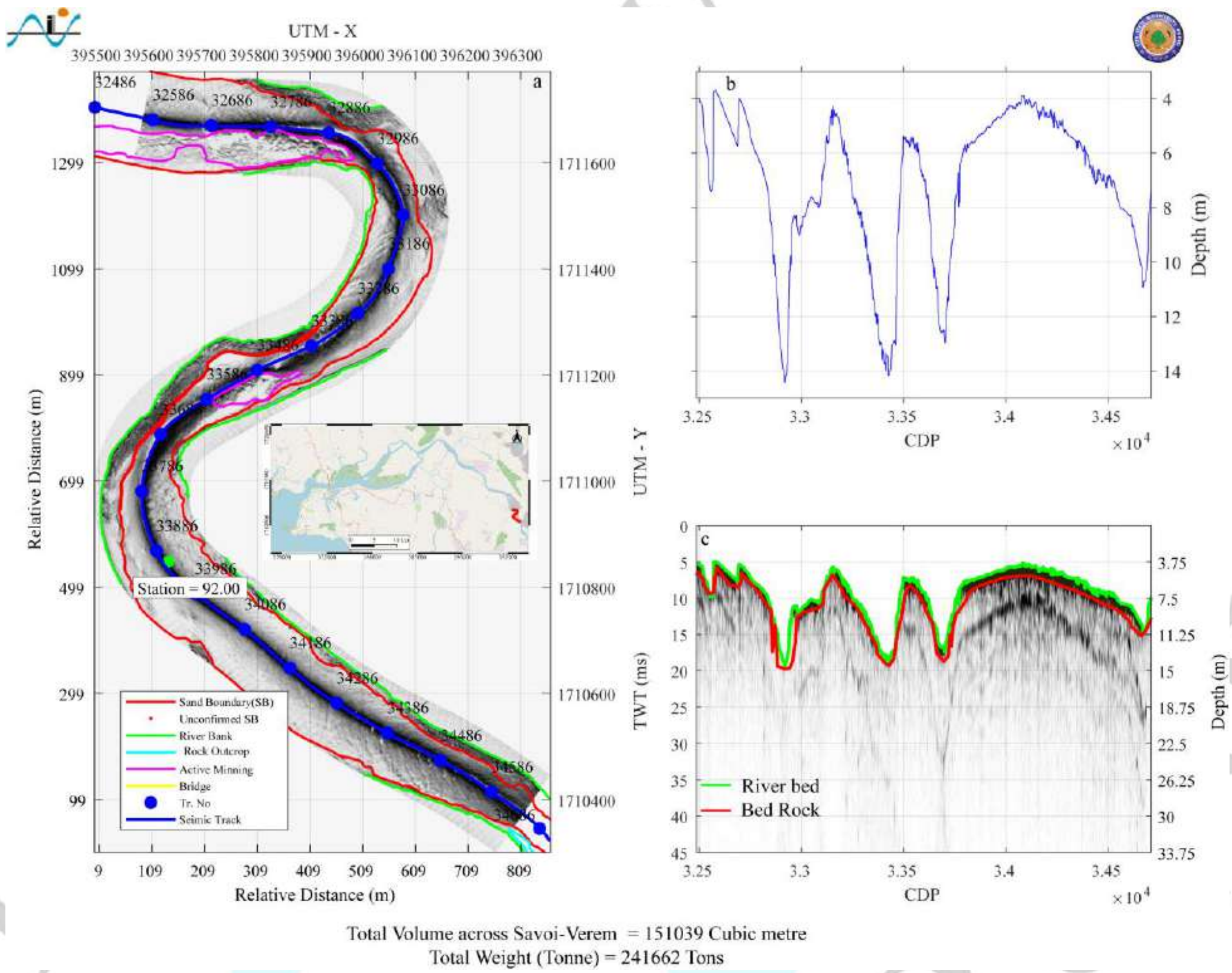

Figure 20. Geophysical data across Khandepar. (a) Side scan sonar (SSS) image (b) single beam echosounder bathymetry. (c) high resolution seismic data

Chapter 5. Geological Observations

Material and Methods

A total of thirty-four surface sediment samples (uppermost 5 cm) covering several parts of the Mandovi River were collected using a hand-held Van Veen grab sampler (Fig. 21). Samples were packed in containers and stored at CSIR-NIO's sample storage repository. The samples are used for Salinity (PPT), pH, Chloride (PPM), sediment nomenclature (grain size through sieving analysis), and microscopic observations for grain sorting, mineral composition and grain angularity.

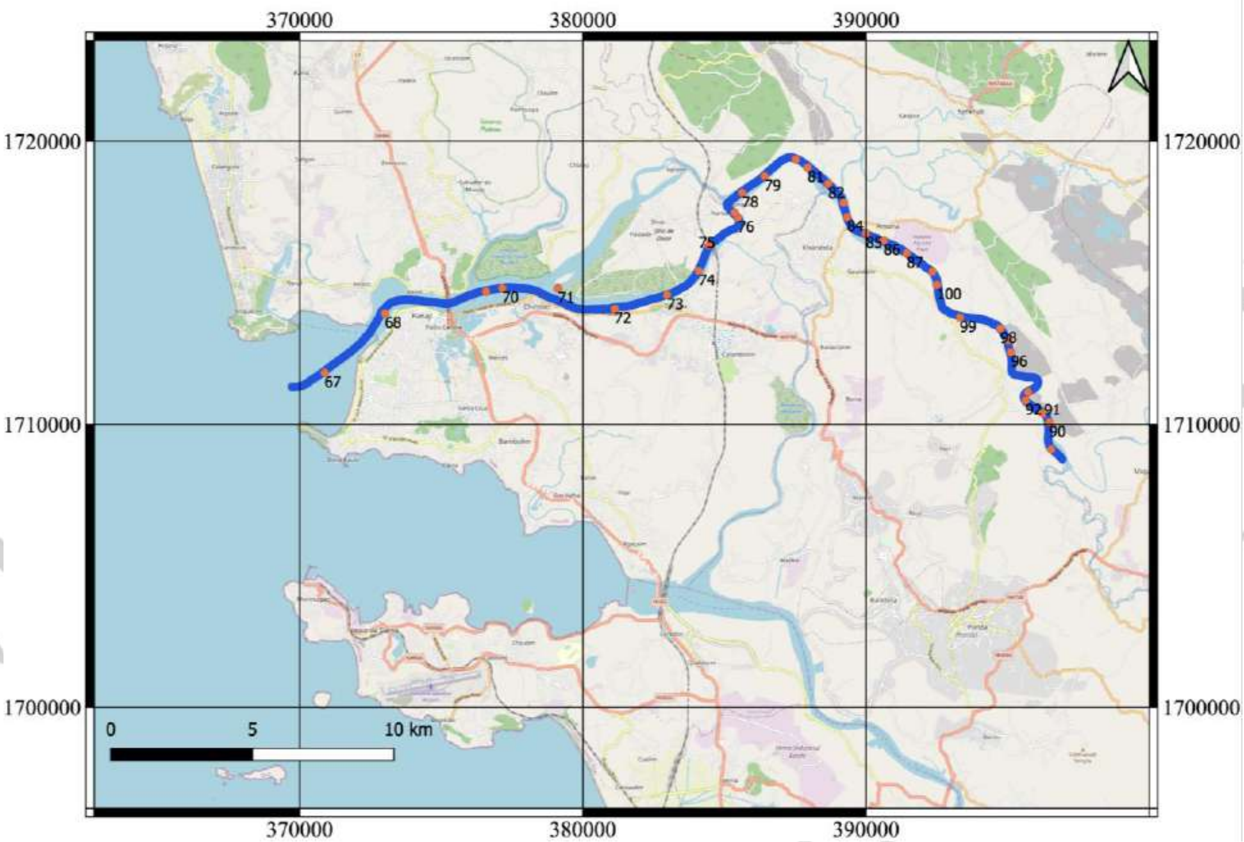

Figure 21. Geological Sample Locations in the Mandovi river.

Sediment Nomenclature

Nomenclature of the Mandovi River sediment samples were done following standard Rock-Color Chart prepared by the Rock-Color Chart Committee (***representing the U.S. Geological Survey, GSA, the American Association of Petroleum Geologists, the Society of Economic Geologists, and the Association of American State Geologists***). The rock color chart for selected stations is provided in Table 2.

Sieve Size analysis

As per IS 650 requirement, bulk sediment samples of about 50 g were dried, weighed, and wet-sieved for 20 mins with an automated sieve shaker (Fritsch Analysette) creating following sieved fractions > 2000 µm, 1600 -2000 µm, 1000 µm ‑ 1600 µm, 850 µm ‑ 1000 µm, 500 µm ‑ 850 µm, 200 µm ‑ 500 µm, and 90 µm – 200 µm. Cumulative percentage passing (%) for nine stations were calculated following ASTM standards are presented in Table 3. Weight percentage of sand and other coarser grains (> 63 µm), silt (4 µm ‑ 63 µm) and clay (< 4 µm) in the Mandovi river sediments are presented in Table 4.

Results

Moderately – well sorted, fine-medium-coarse grained sand is found in majority of the sediment samples from the Mandovi River. The bulk sediment grain size in most of the samples is dominated by sand and other coarser grains fraction. In general, sand and other coarser grains content in the Mandovi River sediments ranges between 91.98 and 100 (wt %), silt content ranges between 0.0 – 4.05 (wt %), and clay content ranges between 0.0 – 6.84 (wt %) (Table 4).

Sampling Station No	**Colour**	**Rock Colour Chart**	**Sorting**
67	Dusky yellowish brown	10YR 2/2	Well sorted
98	Light brown	5YR 5/6	Moderately sorted to well sorted
96	Moderate yellowish brown	10YR 5/4	Poorly sorted
86	Moderate brown	5YR 4/4	Poorly sorted
93	Moderate yellowish brown	10YR 5/4	Cobbles, poorly sorted

Table 2. Nomenclature of Mandovi River (Pre-monsoon) sand samples were done by following standard Rock-Color Chart prepared by the Rock-Color Chart Committee (representing the U.S. Geological Survey, GSA, the American Association of Petroleum Geologists, the Society of Economic Geologists, and the Association of American State Geologists)

STATION NO	Latitude	Longitude	SIEVE SIZE (mm)	SIEVE SIZE (μm)	Cumulative percentage passing (%)
67	15°28'49.40" N	73°47'46.8" E	2	2000	95.02
			1.6	1600	92.2
			1	1000	75.58
			0.85	850	57.2
			0.5	500	31.66
			0.2	200	5.74
			0.09	90	4.06
75	15°31'31.95" N	73°55'09.34" E	2	2000	93.1
			1.6	1600	78.2
			1	1000	63.72
			0.85	850	46.9
			0.5	500	30.96
			0.2	200	9.9
			0.09	90	3.88
82	15°32'29091" N	73°57'42.445" E	2	2000	99.32
			1.6	1600	96.32
			1	1000	95.68
			0.85	850	91.44
			0.5	500	77.9
			0.2	200	32.98
			0.09	90	21.26
86	15°31'24.94" N	73°58'48.65" E	2	2000	97.48
			1.6	1600	94.98
			1	1000	90.78
			0.85	850	85.4
			0.5	500	75.48
			0.2	200	66.26
			0.09	90	31.14
100	15°30'34.25"N	73°59'51.72" E	2	2000	97.26
			1.6	1600	90.92
			1	1000	84.8
			0.85	850	78.48
			0.5	500	68.62
			0.2	200	66.56
			0.09	90	49.08

Table 3 Cumulative percentage of passing of Mandovi River sediment samples as per IS 650 requirements

STATION NO.	LATITUDE	LONGITUDE	Sand and other coarser grains (Wt.%)	Silt (Wt.%)	Clay (Wt.%)
67	15°28’49 40’’ N	73°47’46.80’’ E	99.619565	0.108696	0.0543478
68	15°29’58.14’’ N	73°48’57.83’’ E	99.47644	0.052356	0.104712
69	15°30’23.71’’ N	73°50’57.58’’ E	99.650873	0.099751	0.0997506
70	15°30’27.93’’ N	73°51’16.71’’ E	99.831744	0.056085	0.0560852
71	15°30’27.93’’ N	73°52’22.66’’ E	99.59718	0.20141	0.2014099
72	15°30’04.84’’ N	73°53’30.14’’ E	99.586563	0.05168	0.3100775
73	15°30’20.97’’ N	73°54’32.04’’ E	97.814208	1.967213	0.1639344
74	15°30’48.88’’ N	73°55’09.34’’ E	96.470588	3.284314	0.0980392
75	15°31’31.95’’ N	73°55’09.34’’ E	95.904762	1.952381	1.8095238
76	15°31’50.39’’ N	73°55’55.50’’ E	99.586207	0.137931	0.2298851
77	15°31’56.12’’ N	73°55’51.51’’ E	99.553571	0.089286	0.1339286
78	15°32’18.89’’ N	73°56’00.36’’ E	91.359649	1.666667	6.8421053
79	15°32’38.10’’ N	73°56’26.9’’ E	94.545455	0.512821	4.8951049
80	15°32’57.71’’ N	73°57’03.80’’ E	99.068627	0.588235	0.1470588
81	15°32’48.39’’ N	73°57’17.82’’ E	98.831301	0.965447	0.101626
82	15°32’29.91’’ N	73°57’42.45’’ E	91.981132	4.056604	3.9150943
83	15°32’08.06’’ N	73°58’0.68’’ E	98.968059	0.4914	0.4422604
84	15°31’51.82’’ N	73°58’05.07’’ E	99.319372	0.366492	0.3141361
85	15°31’32.93’’ N	73°58’27.37’’ E	98.898072	0.220386	0.7713499
86	15°31’24.94’’ N	73°58’48.65’’ E	98.564356	0.148515	0.990099
87	15°31’10.29’’ N	73°59’15.94’’ E	97.978723	1.595745	0.1595745
88	15°30’49.20’’ N	73°59’46.38’’ E	99.450549	0.549451	0
89	15°27’25.53’’ N	74°02’08.17’’ E	99.433962	0.283019	0
90	15°27’56.66’’ N	74°02’05.68’’ E	99.460784	0.294118	0
91	15°27’09.68’’ N	74°01’52.46’’ E	100	0	0
92	15°28’21.80’’ N	74°01’37.45’’ E	99.25	0.7	0
93	15°28’31.36’’ N	74°01’40.47’’ E	99.897436	0	0
94	15°28’36.87’’ N	73°01’51.21’’ E	99	0.95	0
95	15°28’49.11’’ N	73°01’40.57’’ E	98.712871	0.742574	0.4950495
96	15°29’ 17.25’’N	74°01’19.97’’ E	99.783784	0.162162	0.0540541
97	15°29’ 30.84’’N	74°01’16.70’’ E	98.690176	0.957179	0.2015113
98	15°29 ‘44.34’’N	74°01’07.17’’ E	97.833753	2.065491	0.1007557
99	15°29’56.66’’ N	74°00’19.29’’ E	96.031746	2.804233	0.6349206
100	15°30’34.25’’ N	73°59’51.72’’ E	99.409091	0.454545	0.0909091

Table 4. Weight percentage of sand, silt and clay fractions in Mandovi River sediments

Microscopic Analysis of geological samples

Methodology

Sand samples collected along the Mandovi river course were air-dried and subsequently treated with 20 ml oxalic acid (0.05M; pH = 0.1) overnight to remove Fe-oxide coatings from the mineral grains. Then the oxalic acid was decanted, and the residual solid was repeatedly washed properly with Mili-q water and dried for microscopic observation. A Leica M205 C microscope was used for the observation. The photomicrographs are attached (Stations 67 to 100)

Salinity and pH

Salinity and pH of the sand samples were measured by using a refractometer (Cole Parmer) and pH meter (Eutech, pH Testr 20), respectively (Table 5). 5g of air-dried sediment samples were washed three times with 25 ml Mili-q water. Salinity and pH were measured for each wash. Refractometer is calibrated by using Milli-Q and pH meter calibrated by using buffer solution of pH values 4, 7, and 10.

Results

1. In most stations, the pH values are above seven, and variations in the pH after washing may be because of leaching out of carbonates and bicarbonates from the sand particles (Table 5).

2. River head locations (station 86 to 100) contains semi-rounded pebbles and large grains of quartz, iron oxides, and lithic fragments. Most of the quartzite is yellowish because of the remnant of the iron oxide coating. The sediment shows well-sorted and highly angular grain distribution from the river mouth to station 81. The grain size range is between 0.05 mm to 0.15 mm (stations 67 to 70). Station 81 to 85 show an admixture of pebbles with fine to medium grain sand. We can observe a decrease in grain size when moving to the river mouth. Most of the stations contain a considerable amount of quartzite, iron oxide, and fewer lithic fragments (Table 6).

Stations	First wash		Second Wash		Third Wash	
	pH	Salinity	pH	Salinity	pH	Salinity
67	8.68	1	8.68	0	8.56	0
68	8.37	0	8.93	0	8.23	0
69	8.19	1	8.56	0	8.47	0
70	7.81	0	8.24	0	7.67	0
71	8.38	1	9.09	0	8.31	0
72	8.28	0	9.22	0	8.24	0
73	9.04	2	9.13	0	8.4	0
74	7.93	1	7.92	0	8.13	0
75	7.83	2	7.86	0	7.36	0
76	7.42	2	7.46	0	7.05	0
77	7.61	2	8.06	0	7.12	0
78	7.59	1	8.04	0	7.56	0
79	7.52	2	7.66	0	7.25	0
80	7.38	1	7.73	0	7.18	0
81	7.26	1	7.43	0	7.47	0
82	7.14	2	7.45	0	7.26	0
83	7.09	1	7.55	0	7.4	0
84	7.65	1	7.83	0	7.37	0
85	7.83	0	7.52	0	6.86	0
86	7.2	1	7.47	0	7.23	0
88	7.44	1	7.88	0	7.45	0
89	7.13	2	7.29	0	8.3	0
90	6.86	1	6.59	0	6.79	0
91	7.34	2	7.84	0	7.21	0
92	6.98	1	7.27	0	7.46	0
93	6.94	0	7.13	0	6.45	0
94	7.64	2	8.24	0	7.11	0
95	7.07	1	6.96	0	6.9	0
96	6.98	1	7.76	0	6.96	0
97	7.07	0	7.85	0	7.09	0
98	7.33	0	7.63	0	7.07	0
99	6.46	2	7.09	0	6.72	0
100	7.26	1	7.2	0	7.45	0

Table 5. The pH and salinity variation of the sand samples for 3-stage fresh water washing.

Photomicrographic images of dry sediments

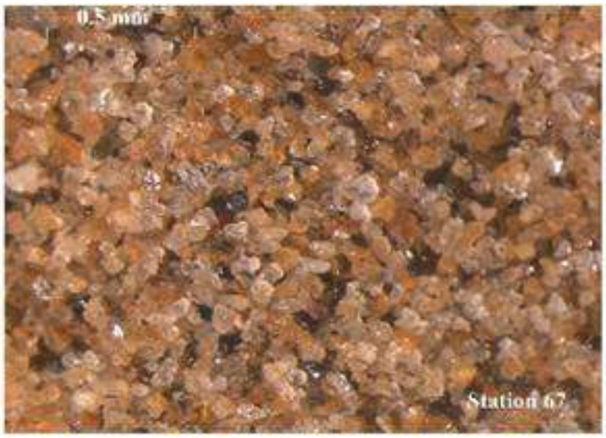

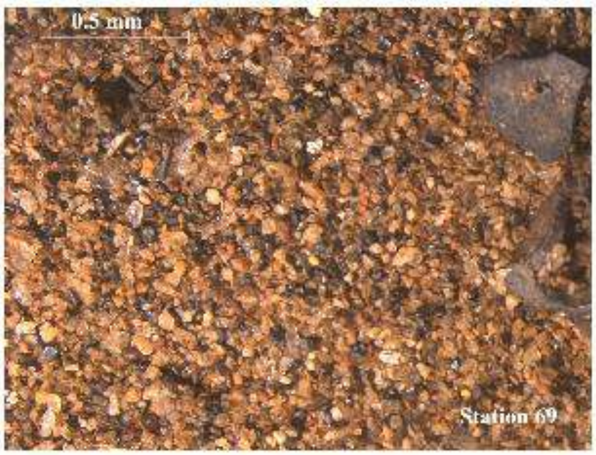

Continued..


0.5 mm
Station 73

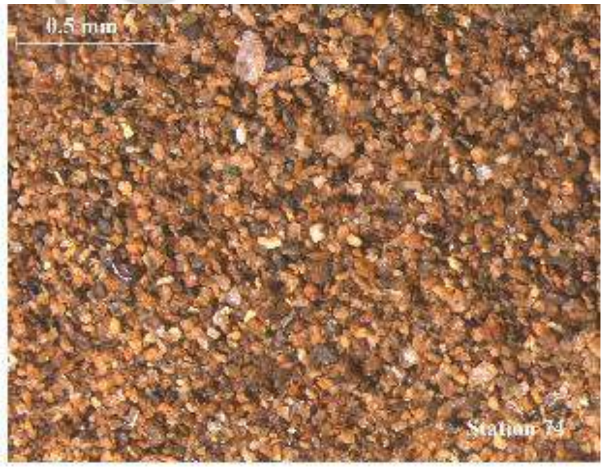
0.5 mm
Station 74


0.5 mm
Station 75


0.5 mm
Station 76

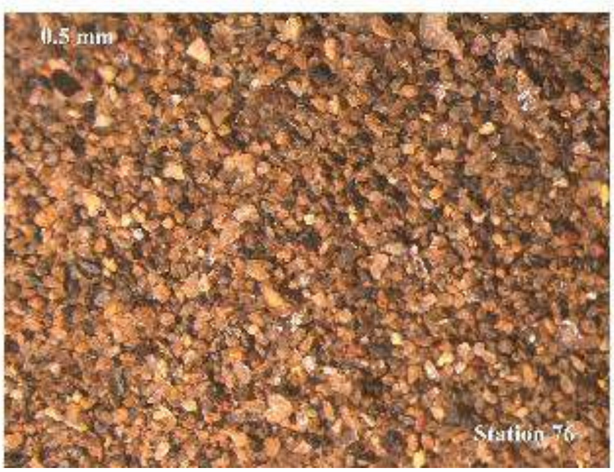
0.5 mm
Station 76

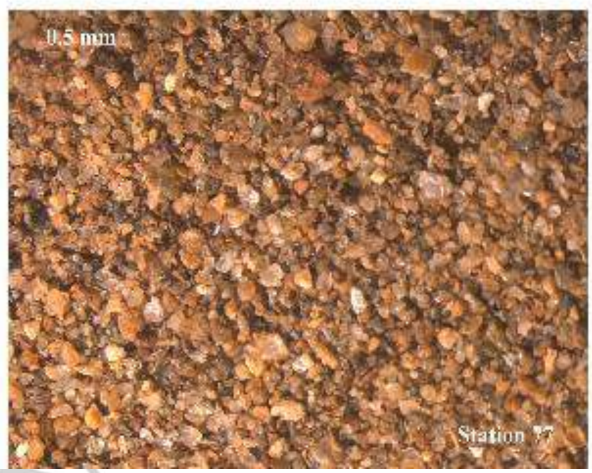
0.5 mm
Station 77

Continued..


0.5 mm
Station 78


0.5 mm
Station 79


0.5 mm
Station 80


0.5 mm
Station 81


0.5 mm
Station 82


0.5 mm
Station 83

Continued..


0.5 mm
Station 84


Station 85


0.5 mm
Station 86


0.5 mm
Station 88


0.5 mm
Station 89


0.5 mm
Station 90

Continued..


0.5 mm
Station 91


0.5 mm
Station 92


0.5 mm
Station 93


0.5 mm
Station 94


0.5 mm
Station 95


0.5 mm
Station 96

Continued..

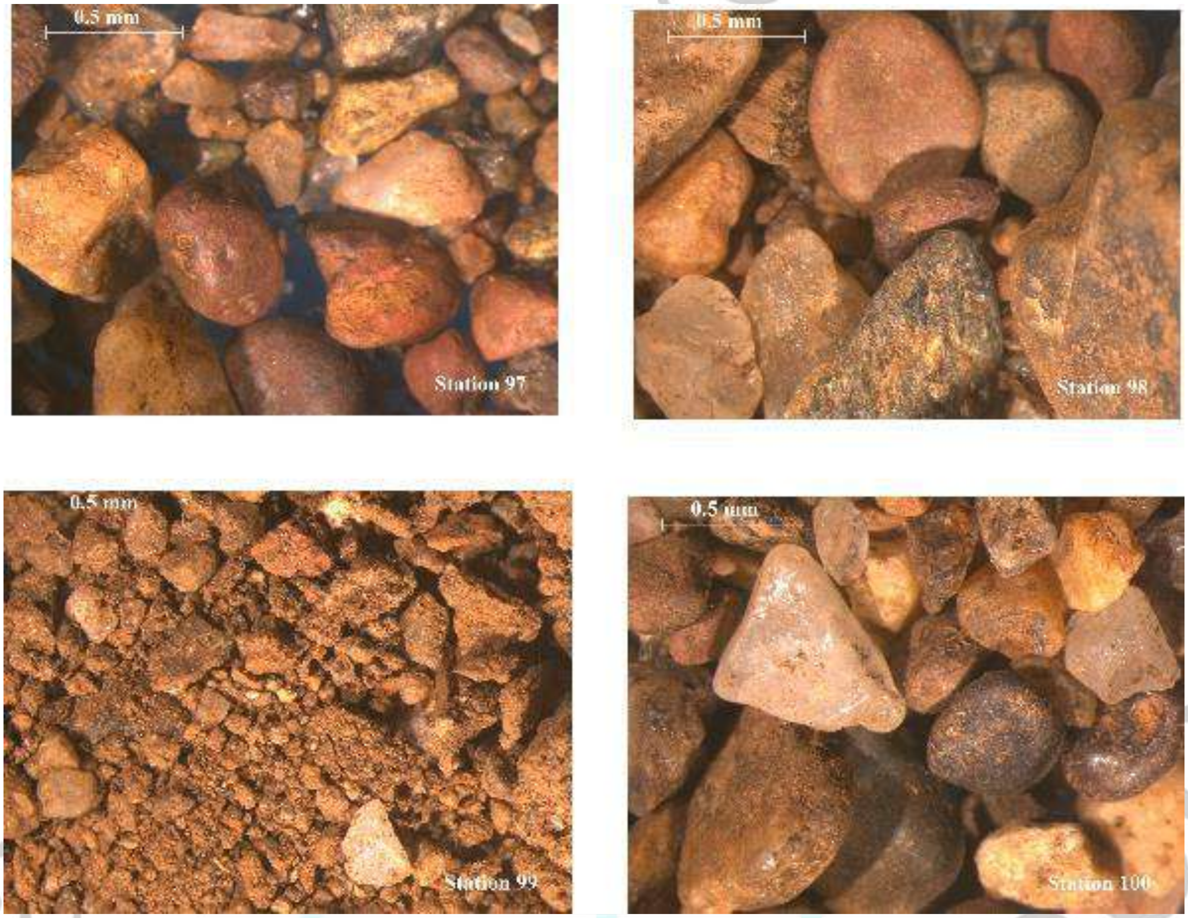

Figure 22. Microscopic Images of Geological Samples

Mandovi	**Large grain size(mm)**	**Small grain size(mm)**	**Remarks**
Station 67	0.15	0.05	Well sorted, highly angular quartz, rounded to semi-rounded iron oxide
Station 68	0.15	0.05	Well sorted, highly angular quartz, rounded to semi-rounded iron oxide
Station 69	0.15	0.04	Angular quartz rounded to semi-rounded iron oxide
Station 70	0.175	0.05	Highly angular quartz, rounded to semi rounded iron oxide
Station 71	0.275	0.05	Different size of grains, iron oxide, angular quartz
Station 72	0.535	0.05	Highly angular quartz, rounded to semi rounded iron oxide
Station 73	0.879	0.05	Highly angular quartz, rounded to semi rounded iron oxide, poor sorting
Station 74	0.170	0.05	Quartz and iron oxides present, sorting improved compare to station 73.

Station 75	0.180	0.05	Quartz and iron oxides present, sorting improved compare to station 73.
Station 76	0.180	0.05	Quartz and iron oxides present, sorting improved compare to station 73.
Station 77	0.180	0.05	Quartz and iron oxides present, sorting improved compare to station 73.
Station 78	0.180	0.05	Quartz and iron oxides present, sorting improved compare to station 73.
Station 79	0.180	0.05	Quartz and iron oxides present, sorting improved compare to station 73.
Station 80	0.658	0.075	Quartz, lithic fragments, rounded iron oxides, large grain size
Station 81	0.225	0.05	Quartz, rounded to semi rounded iron oxides
Station 82	0.312	0.05	Iron oxides, quartz occurred along with mud.
Station 83	0.914	0.05	Quartz, iron oxides, rock fragments
Station 84	1.7	0.06	Quartz, iron oxides, poorly sorted
Station 85	0.262	0.07	Quartz, iron oxides along with mud.
Station 86	25	0.05	Very large grains of quartzite and iron oxide
Station 88	0.35	0.03	Quartzite and iron oxide
Station 89	30	0.075	Very large grains of quartzite and iron oxides
Station 90	20	10	Very large grains only
Station 91	20	0.1	Large angular grains, quartzite, lithic fragments, rounded iron oxide
Station 92	33	0.10	Very large grains, quartzite, Iron oxides
Station 93	30	0.12	Quartzite, Iron oxides, lithic fragments
Station 94	0.941	0.03	Quartzite, Iron oxides, wood fragments, mud
Station 95	28	0.5	Very large grains, angular quartzite, Iron oxides
Station 96	13	0.1	Large gains, quartzite, rounded iron oxides, lithic fragments
Station 97	30	0.15	Very large grains, quartzite, rounded to semi rounded iron oxides
Station 98	25	0.1	Very large grains, quartzite, rounded to semi rounded iron oxides
Station 99	0.35	0.1	Angular, iron oxides, mud
Station 100	17	0.1	Large grains, quartzite, iron oxides, rock fragments

Table 6. Detailed microscopic observation of sand samples

Chapter 6. Post Monsoon Geophysical Survey

Geophysical data acquisition:

The post monsoon geophysical data comprising Side scan sonar (SSS), high resolution seismic (HRS) and Single beam echo-sounding data have been acquired in the Mandovi river, north Goa to observed any post-monsoon geomorphological and subsurface changes. The analysis of the geophysical data provides information about new sediment deposition or erosion of river bed as well as replenishment of the pre-existing mining zones.

Major features identified from the side scan sonar (SSS) imaging and high resolution seismic (HRS):

Riverbed morphology through the side scan sonar images have been carefully analysed in order to infer the river bed geomorphological changes after the monsoon, and high-resolution seismic imaging is carried out to study the changes in sediment thickness, if any after monsoon. The post-monsoon side scan sonograms, high resolution seismic sections have been analysed and compared with respective pre-monsoon data (collected during March 2020) for any major geomorphological changes.

Seismic Data Interpretation:

The difference between the river bed and basement or any other subsurface reference reflector interpreted from the pre-monsoon and post monsoon high resolution seismic data is studied to identify the locations of sediment aggradation/degradation of the river bed in the Mandovi river. The analysis revealed insignificant to significant aggradation/degradation of the river bed through the Mandovi River course. The aggradation/degradation of the river is small and localised and probably suggests local adjustment of the river. In the present report, data representing few regions are highlighted. Figs. 23a, b highlights the pre- and post-monsoon seismic data acquired between Panaji bridge and Ribandar ferry point in the Mandovi river. Comparison of both the seismic sections (a and b) do not reveal any significant change in the basement, riverbed and subsurface reflectors. Whereas Fig. 23c highlights sediment thickness obtained from above two seismic sections. Except some places, sediment thickness doesn’t show any significant variations between pre- and post-monsoon survey. At few places, it varies between ~ 0.3 and 0.4 m. Figs. 24a, b highlights the pre- and post-monsoon seismic data acquired near Narve village. Comparison of the seismic sections show changes in the riverbed and subsurface reflectors whereas no considerable change in the interpreted basement. Fig.24c highlights sediment thickness variations obtained from above two seismic sections. It shows aggradation of riverbed in this region. The increase of sediment thickness is ~0.5 to 1.0 m except at few locations where it reaches up to ~ 2.0 m. Figs. 25a,b highlight the pre- and post-monsoon seismic data acquired near Piligao ferry point. Though the basement reflector doesn’t show any considerable change, the riverbed and embedded reflectors show some identifiable changes at points. Formation of a new lenticular facies can be easily observed at around 700 to 1000 m relative distance. Fig.25c highlights sediment thickness variations obtained from pre- and post-monsoon seismic data. It shows degradation of the riverbed in upstream region and an aggradation of the riverbed in downstream region. The degradation and aggradation both varies between 0.5 m to 2.0 m at their respective regions. Figs. 26a,b highlight the pre- and post-monsoon seismic data acquired near the Vedanta pig Iron plant, Navelim and Fig. 26c highlights sediment thickness variations obtained from pre- and post-monsoon seismic data. It shows a noticeable localized aggradation in riverbed to the order of ~0.30-0.40 m across the region.

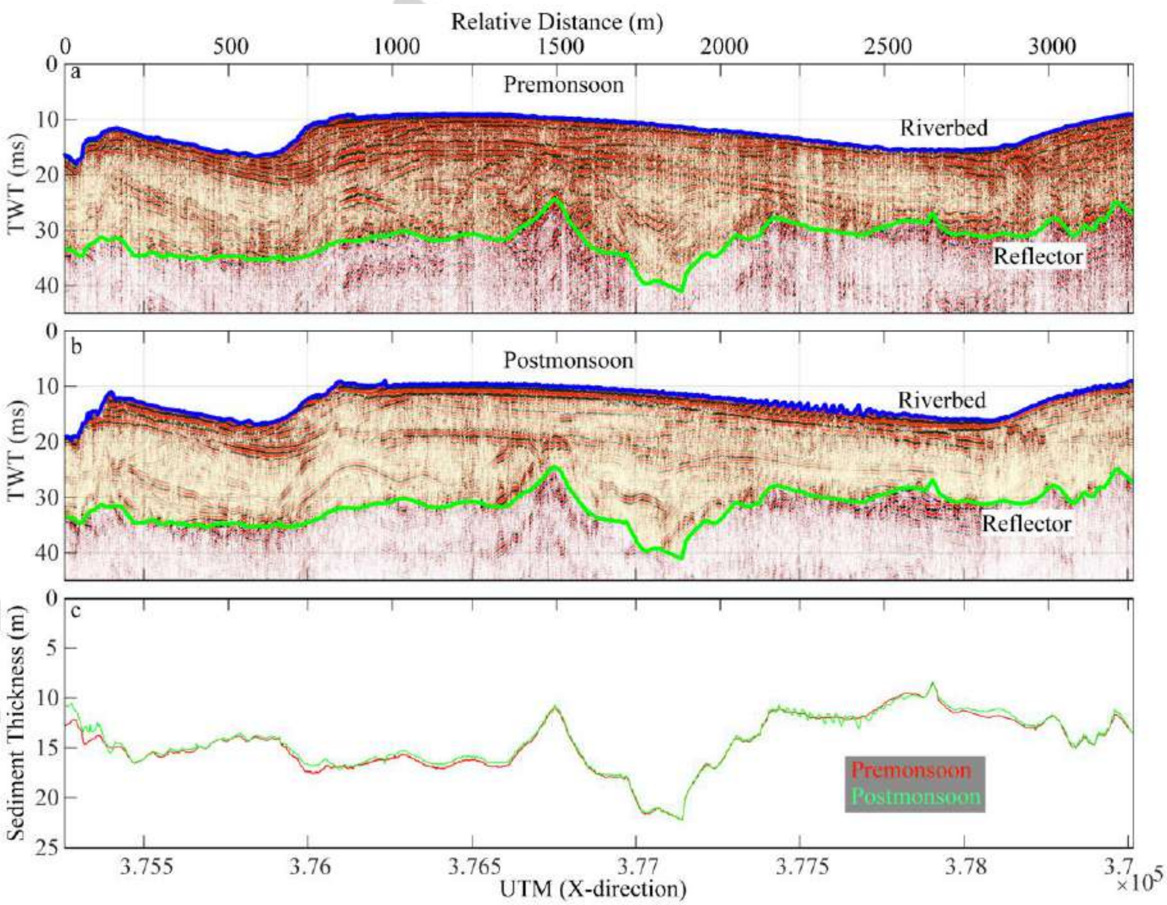

Figure 23. High resolution seismic data. a) pre-monsoon seismic data, b) post-monsoon seismic data, c) sediment thickness across Panaji to Ribandar village

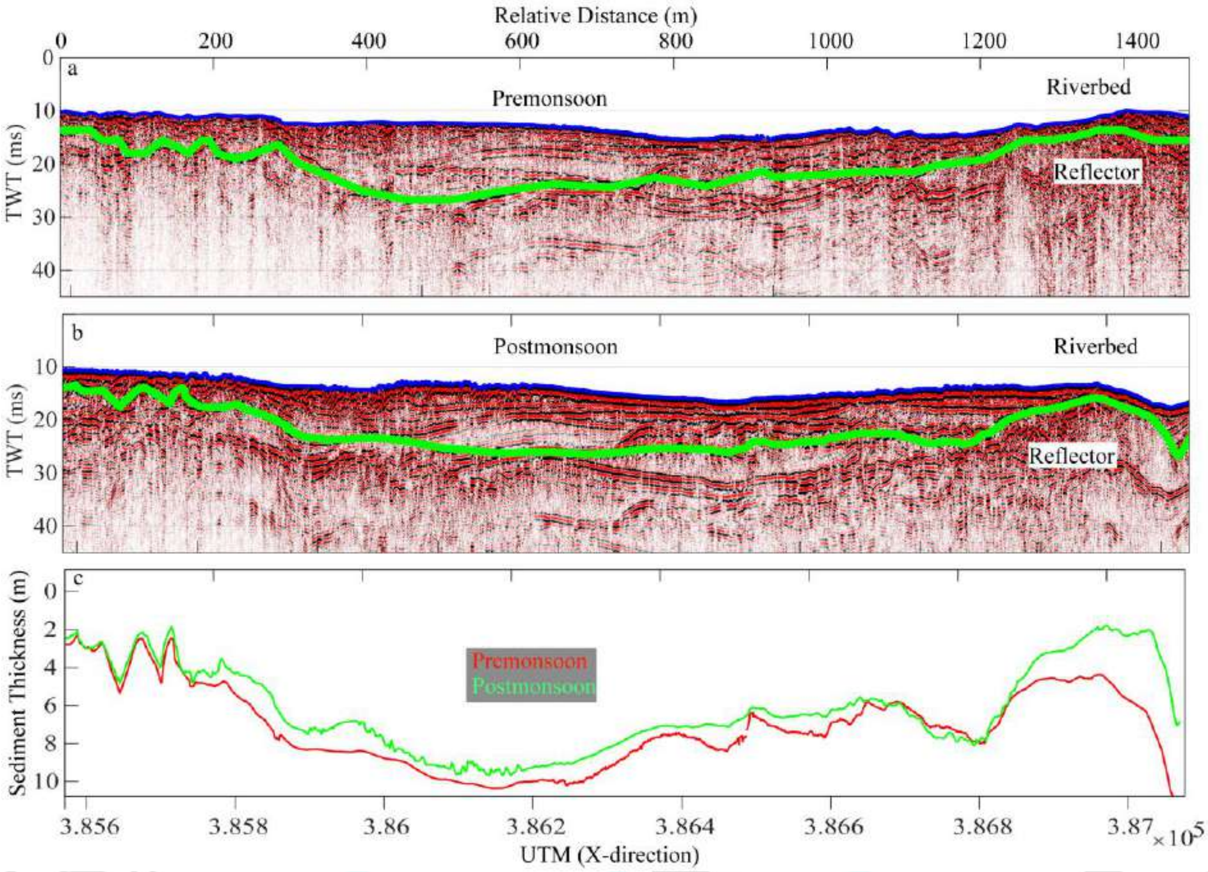

Figure 24. High resolution seismic data. a) pre-monsoon seismic data, b) post-monsoon seismic data, c) sediment thickness across Narve village

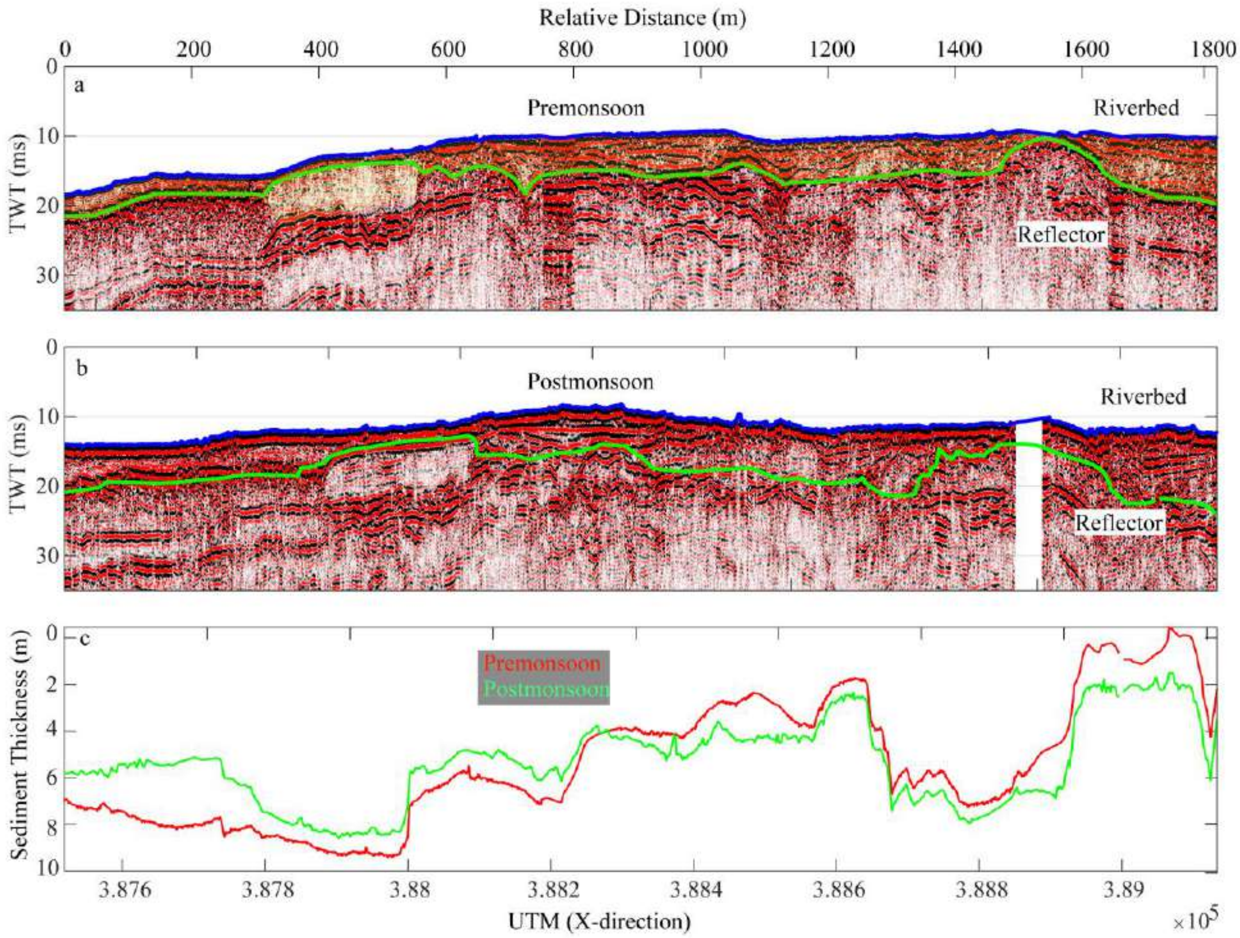

Figure 25. High resolution seismic data. a) pre-monsoon seismic data, b) post-monsoon seismic data, c) sediment thickness across Piligao ferry point

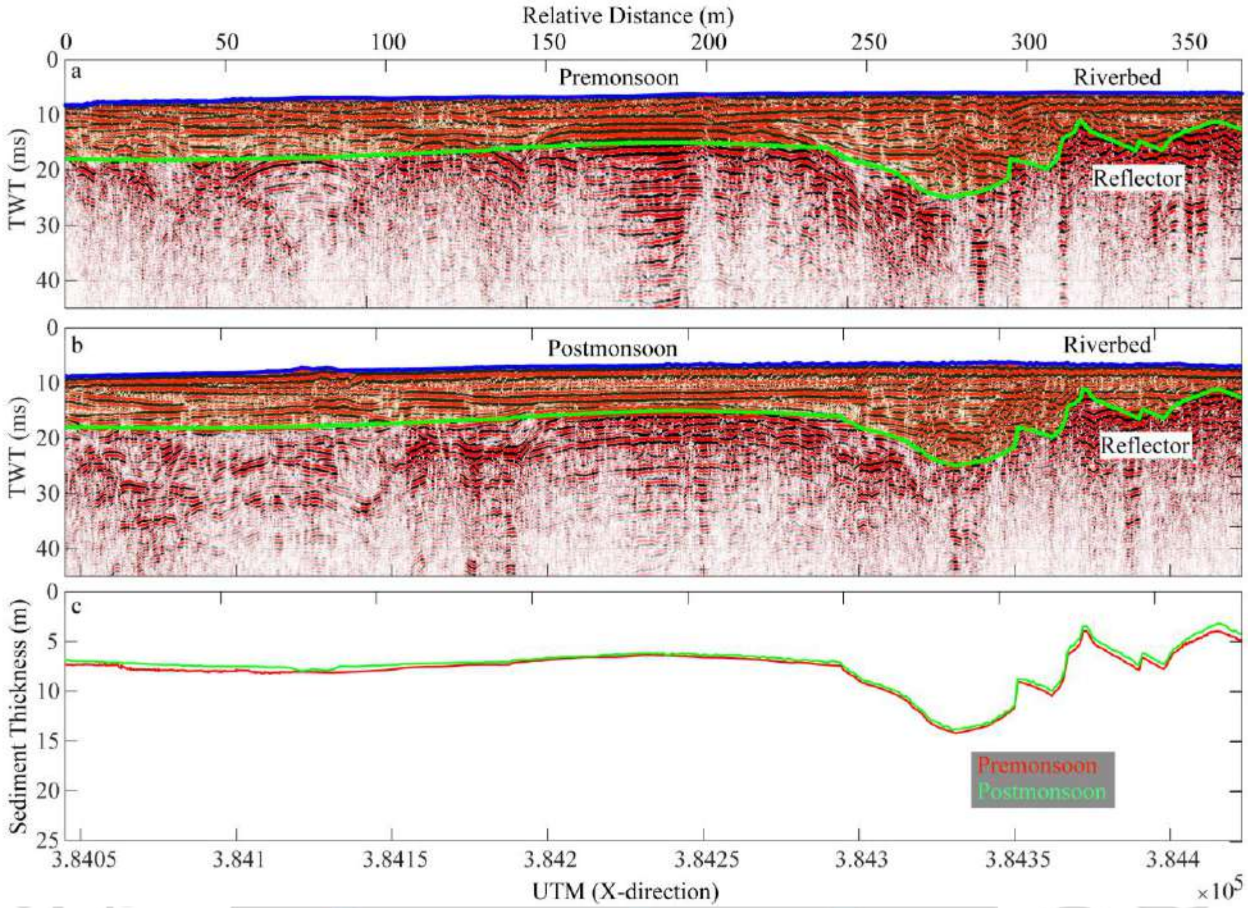

Figure 26. High resolution seismic data. a) pre-monsoon seismic data, b) post-monsoon seismic data, c) sediment thickness across Vedanta pig Iron plant, Navelim

Side Scan Sonar Interpretation

The side scan sonar data provides the regional riverbed morphology across the river and a time lag comparison of side scan sonograms may reveal significant information about ongoing river bed morphology changes at a local scale. A detailed comparative analysis of the pre-monsoon and post-monsoon side scan sonograms have been carried out to identify river bed morphological changes throughout the Mondovi River. The analysis revealed several morphological changes such as mid-channel/point bars erosion, deposition of non-cohesive sediments, washing out of old mining signatures and change in mining pattern. Few representative morphological variations are presented in this report. Fig. 27 highlights the pre- and post-monsoon side scan sonograms near Narve village. Fig. 27a,b shows mining signatures during pre-monsoon and post-monsoon seasons, respectively. A complete wash out of old sand mining signatures and some new mining locations are observed. Fig. 28a highlights the pre-monsoon mining signatures and rock outcrops observed near the Amona bridge and Fig. 28b shows mining signatures during post monsoon period. Old mining signature are completely obliterated and some new mining signatures are observed. Fig. 29a shows side scan sonar images near Navelim-Betqi region. Fig. 29a,b shows mining signatures and rock outcrops during pre-monsoon and post-monsoon seasons, respectively. A complete wash out of old sand mining signatures and some new mining locations are observed. Fig. 30 highlights side scan sonar images near the Navelim-Volvoi region. Fig. 30a depicts presence of a bank bar and type-2 mining signatures, whereas Fig. 30b shows partially eroded sand bar and new set of type-2 mining signatures. Old mining signatures are completely replenished. Sand bar erosion and replenishment of the mining area indicates local redistribution of sediment. Fig. 31 highlights pre- and post-monsoon side scan sonogram acquired near Cotombi-Savoi Verem region. Fig. 31a depicts a point bar, a mid-channel bar, type-1 mining signature and rock outcrops, whereas Fig. 31b depicts a partially eroded point bar and type-2 mining signature along with rock outcrops. In Fig. 31b, partial erosion of point bar and mid-channel bar along with complete wash out of old sand mining signature indicate local redistribution of sediment. Fig. 32 shows side scan sonogram acquired near Khandepar-Vagurme region. Fig. 32a highlights a sediment lag and a mid-channel bar during the pre-monsoon period. The sediment lag and mid-channel bar in Fig. 32a A are completely eroded and not present in the Fig. 32b.

The morphological changes such as bar thinning, lag removal and complete wash out of sand mining signatures, indicate ongoing erosion and deposition processes in the upstream region of the river. SSS data revealed deposition of the “removed sediment” in the immediate downstream vicinity. This indicates local redistribution of the sediment predominantly in downstream section. Morphological changes are not prominent downstream Navelim, except the change in mining signatures and pattern. The complete wash out of old mining signature in these regions suggests either new sediment deposition or local reworking of the sediment or both. Comparison of seismic data at selected locations reveals that local reworking with a small amount of new sediment entrainment from upstream have taken place in the Navelim-Betqui to Narve regions. The sediment load from the Valvanti River may also contribute to the sediment deposition between Piligao and Narve regions.

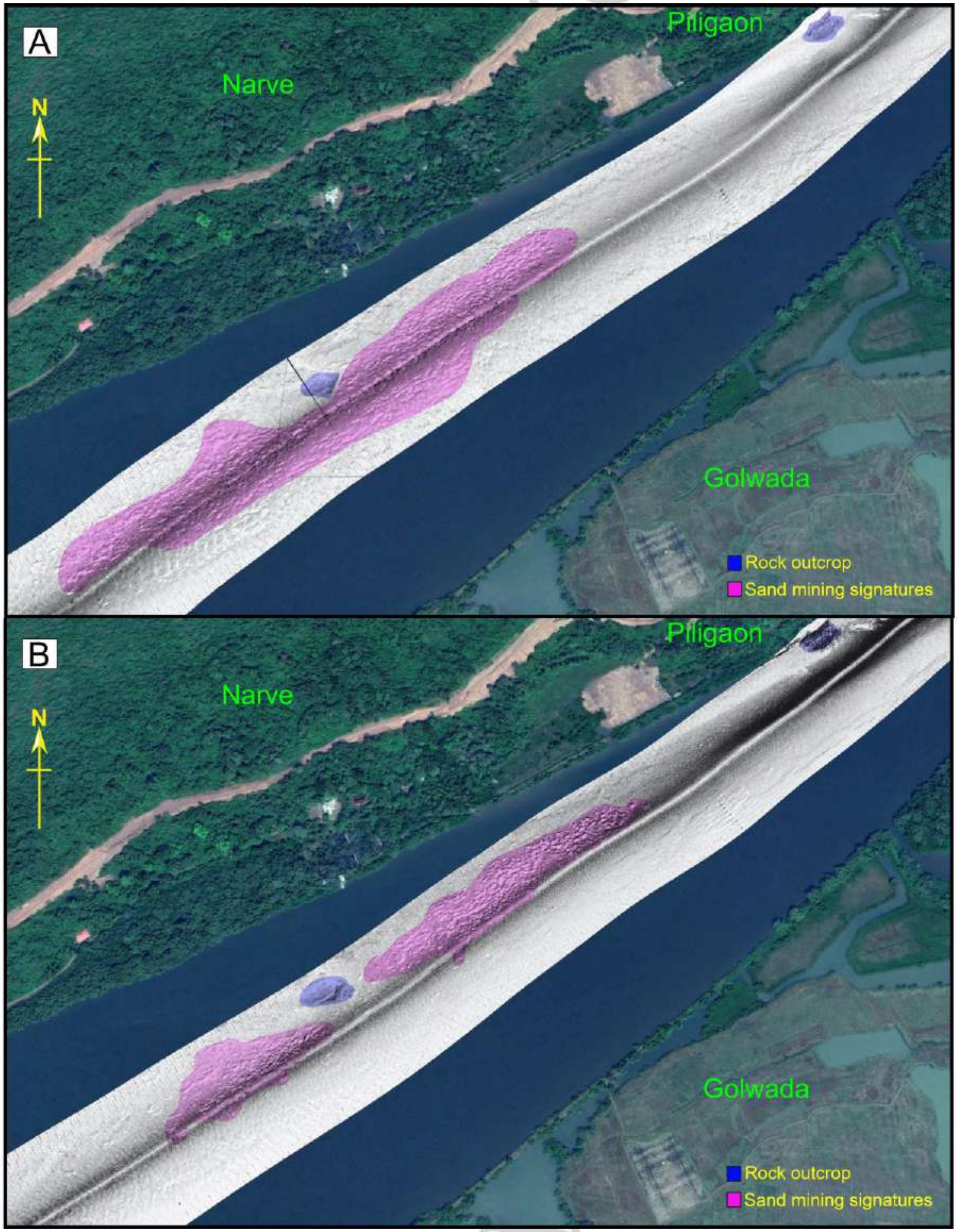

Figure 27. Side Scan Sonograms acquired near Narve village during (A) pre-monsoon and (B) post-monsoon seasons. (A) and (B) both show the presence of sand mining signature and change in mining pattern. of type-1.

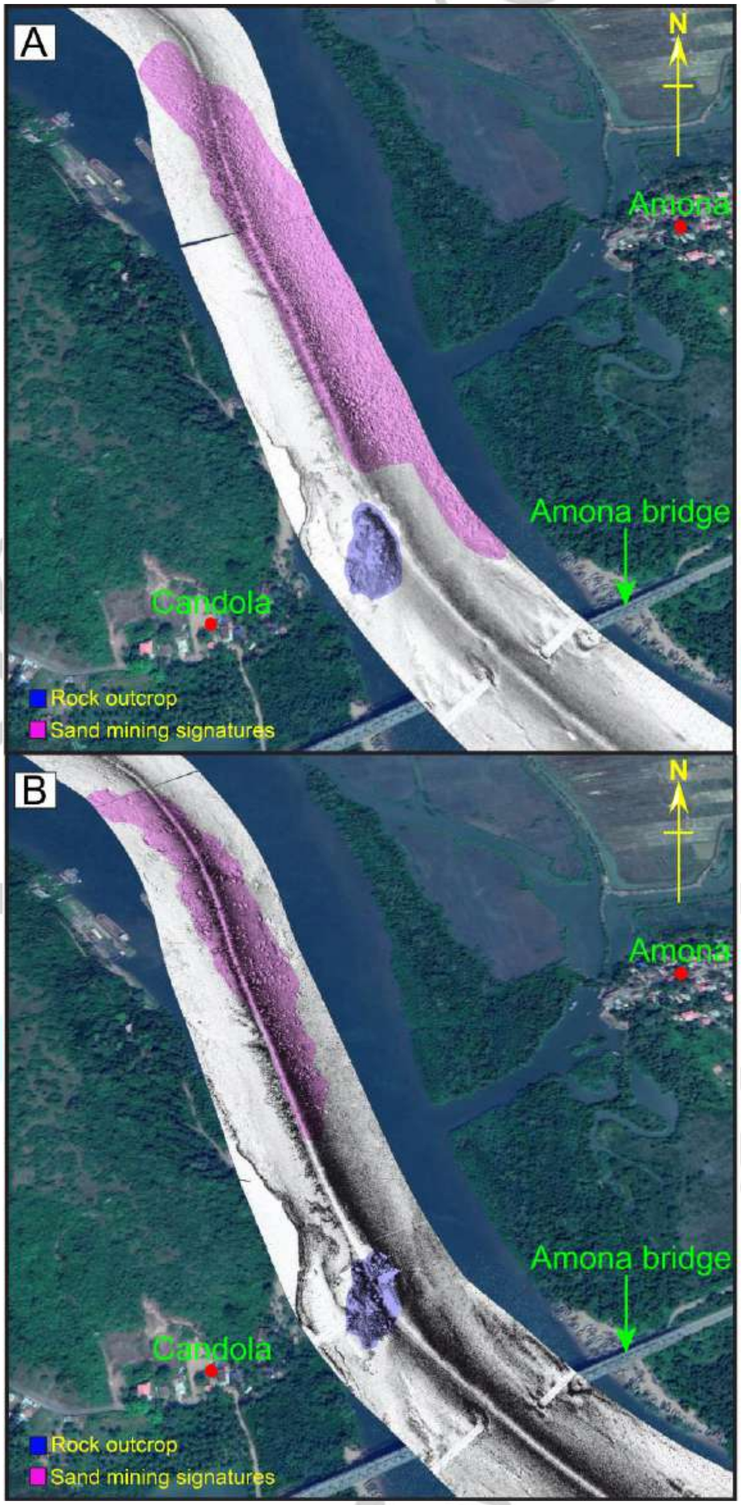

Figure 28. Side Scan Sonograms acquired near downstream Amona bridge (A) pre-monsoon and (B) post-monsoon seasons. (A) and (B) primarily highlight sand mining signatures and change in mining patterns. Both show the presence of sand mining signature of type-1.

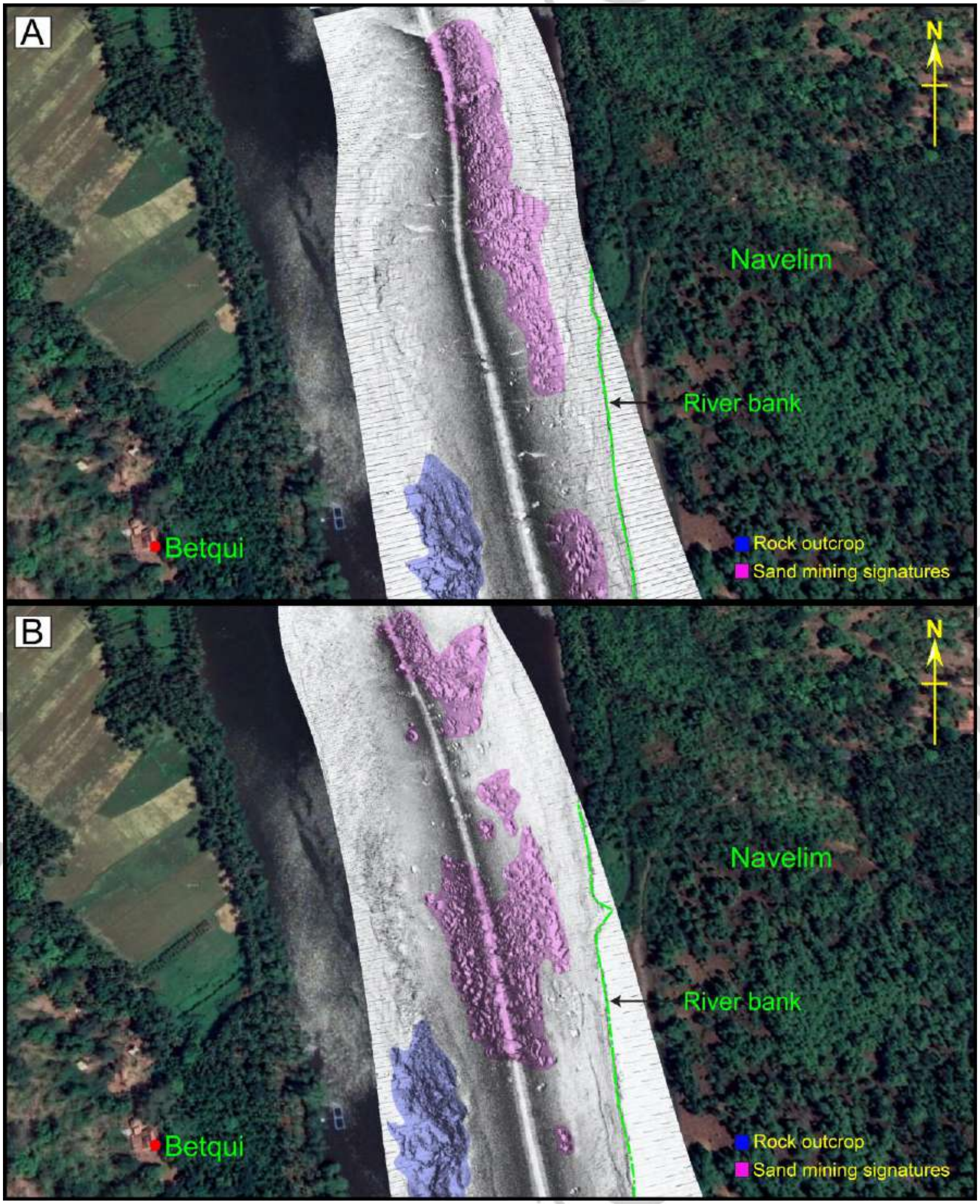

Figure 29.Side Scan Sonogram acquired near Navelim-Betqi region during (A) pre-monsoon and (B) post-monsoon seasons. (A) and (B) both show riverbed morphology along with rock outcrop and sand mining signatures. (A) and (B) highlight change in sand mining patterns

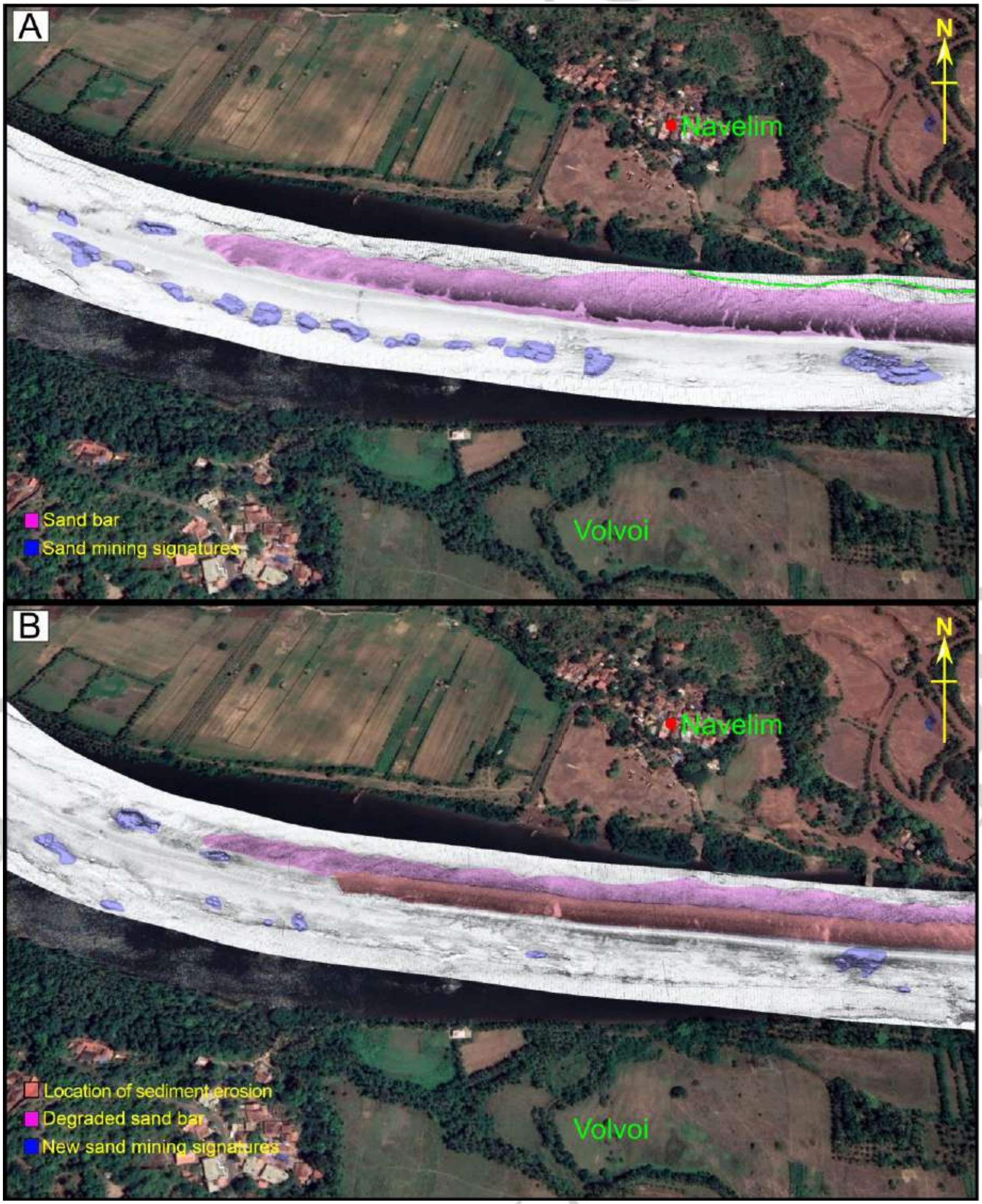

Figure 30.Side Scan Sonogram acquired in Navelim-Volvoi region during (A) pre-monsoon and (B) post-monsoon seasons. (A) Along with river bed morphology, it shows presence of sand bar and sand mining signatures of type-2. (B) highlights partial erosion of the sand bar and replenishment of old mining signatures.

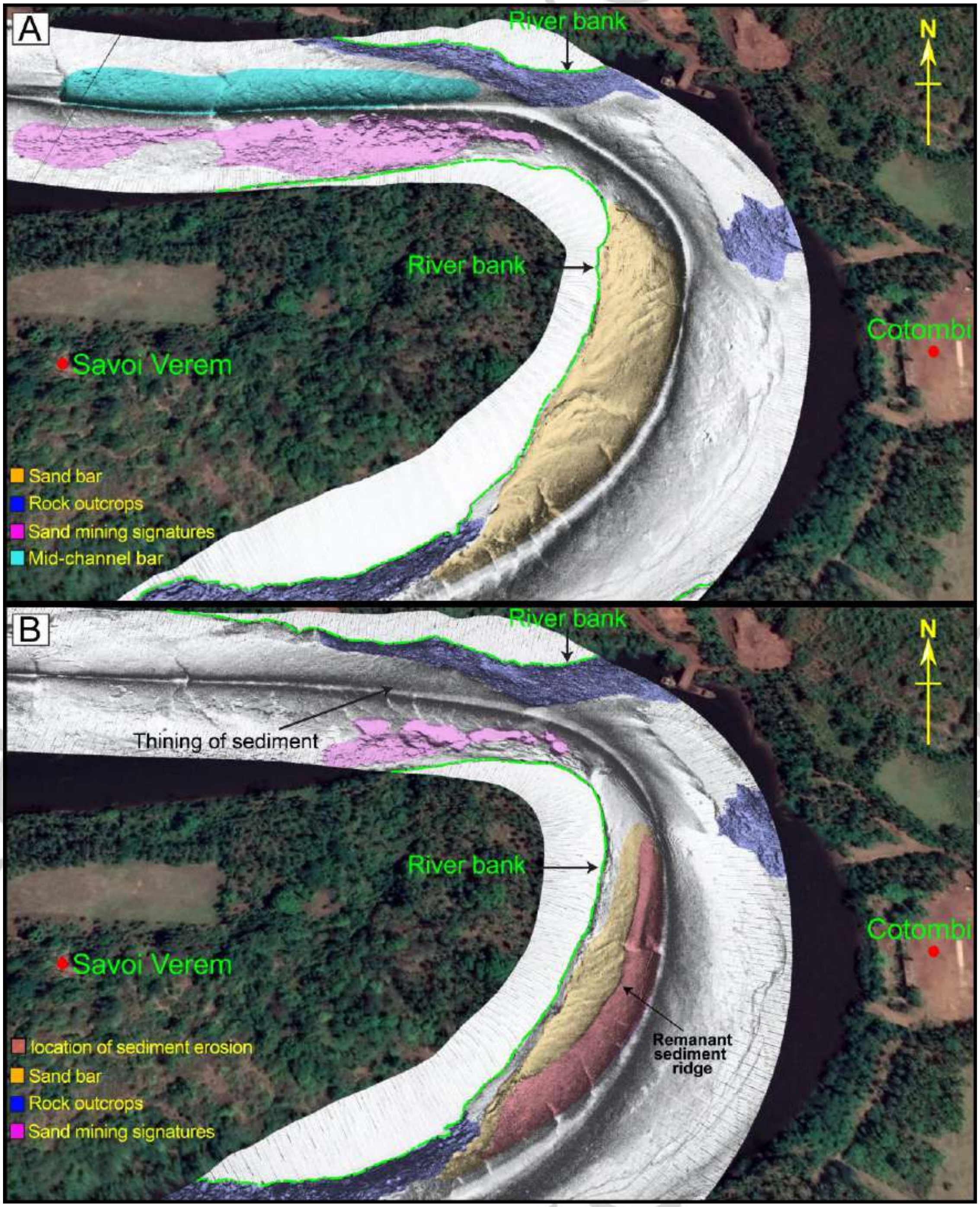

Figure 31. Side Scan Sonogram acquired between Savoi Verem-Cotombi region during (A) pre-monsoon and (B) post-monsoon seasons. (A) Shows presence of point bar and mid-channel bar along with sand mining signatures on the river bed and (B) highlights partial erosion of point bar and thinning of the mid channel bar. Its also highlights the change in sand mining activity.

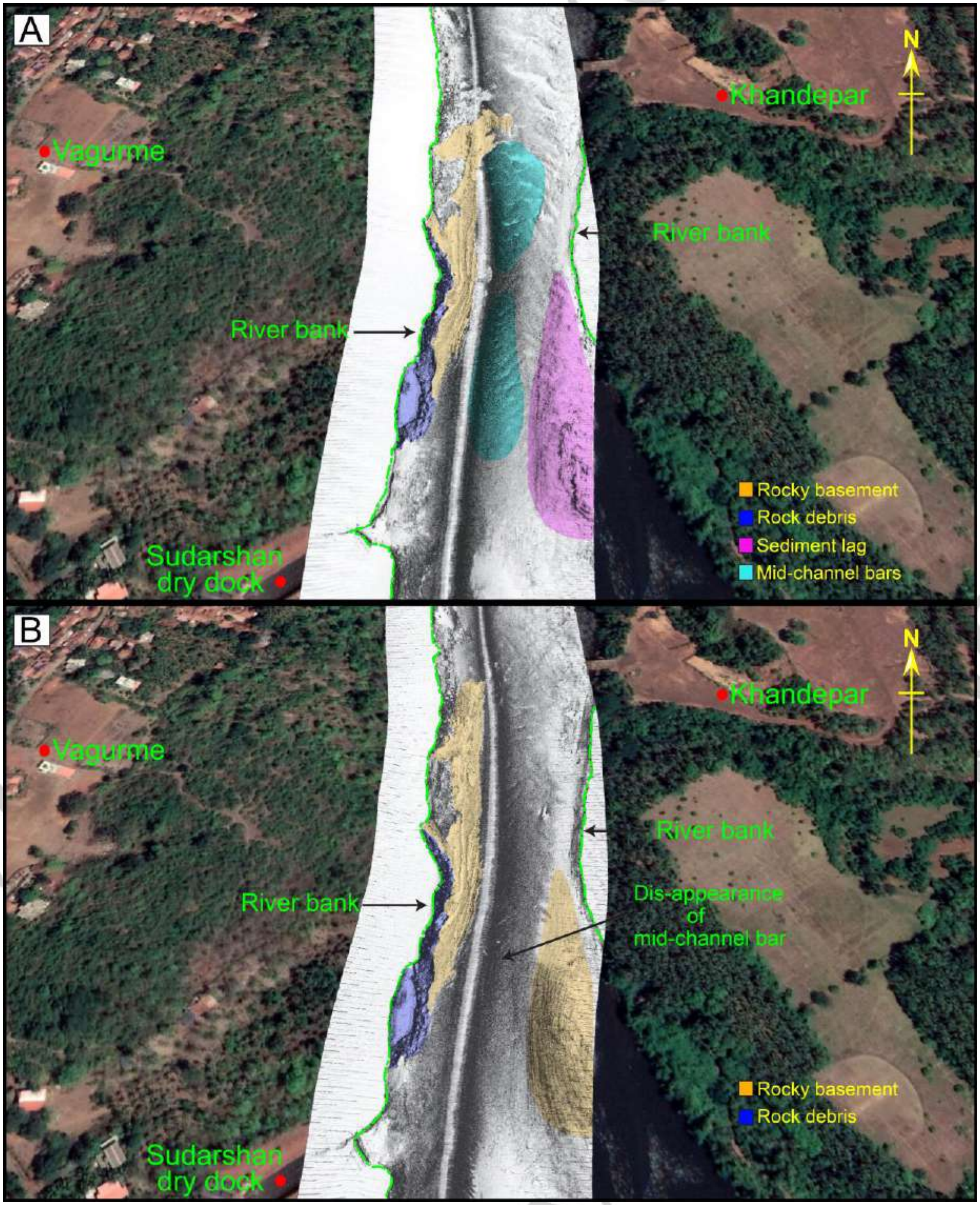

Figure 32. Side Scan Sonogram acquired in Khandepar-Vagurme region during (A) pre-monsoon and (B) post-monsoon seasons. The sonograms highlight removal of bank sediment lag and thinning of mid-channel bar.

Chapter 7. Conclusions

Based on the side scan sonar imaging, single beam echosounder bathymetry and high resolution seismic (HRS), morphological features of river bed have been interpreted across a stretch of 38 km of Mandovi river. The side scan sonar image shows various geomorphological features like ripple marks (associated with sand), rock outcrops, river banks, erosion features, mud zones and shadow zones of the road and railway bridges across the Mandovi river. Apart from this, active mining zones in different regions of Mandovi river are also identified. The single beam echo sounding data is used for estimating the real-time depth of the river bed and the high-resolution seismic data is utilized for the estimating the subsurface structure and sediment thickness.

The microscopic grain size analysis shows a decrease in grain size when moving from Khandepar to the river mouth. The bulk sediment grain size in most of the samples is dominated by sand and coarser fractions. Most of the stations contain a considerable amount of quartzite, iron oxide, and fewer lithic fragments. Based on the analysis, the region is divided into three zones. Zone1: Khandepar to Navelim (sampling point 86-100), characterised by poorly sorted, semi rounded pebbles and large grain size sediments along with silt clay pockets; Zone2: Piligao to Navelim (sampling points 81-85), characterised by poor to moderately sorted, admixture of pebbles and fine to medium grain sand and Zone3: River mouth to Piligao (sampling point 67-81), characterised by well-sorted and highly angular grain distribution (Fig. 33).

The comparative analysis reveals that Khandepar, Cotombi, Volvoi, Navelim, and Betqi, are the locations where mid-channel/point bars erosion and deposition of non-cohesive sediments in the nearby downstream region is prominent. Whereas, Navelim-Betqui, Amona, Piligaon, Narve are the regions where the morphological changes are not prominent, except the variations in mining signatures and patterns. Integrated analysis of SSS and HRS data at respective locations revealed that a local redistribution of the sediment is happening in most of the region.

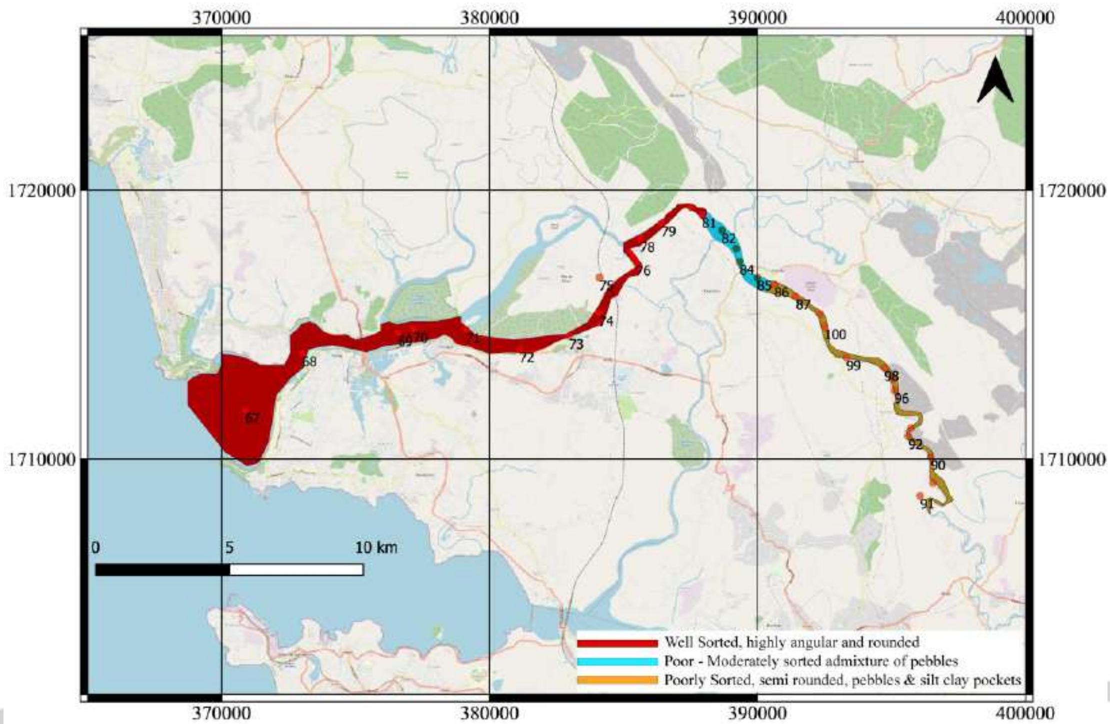

Figure 33. Sand sediment grain size distribution from upstream to river mouth

Based on the studies and EIA/EMP, possible mining regions have been identified and given below.

Zones 1 – 2

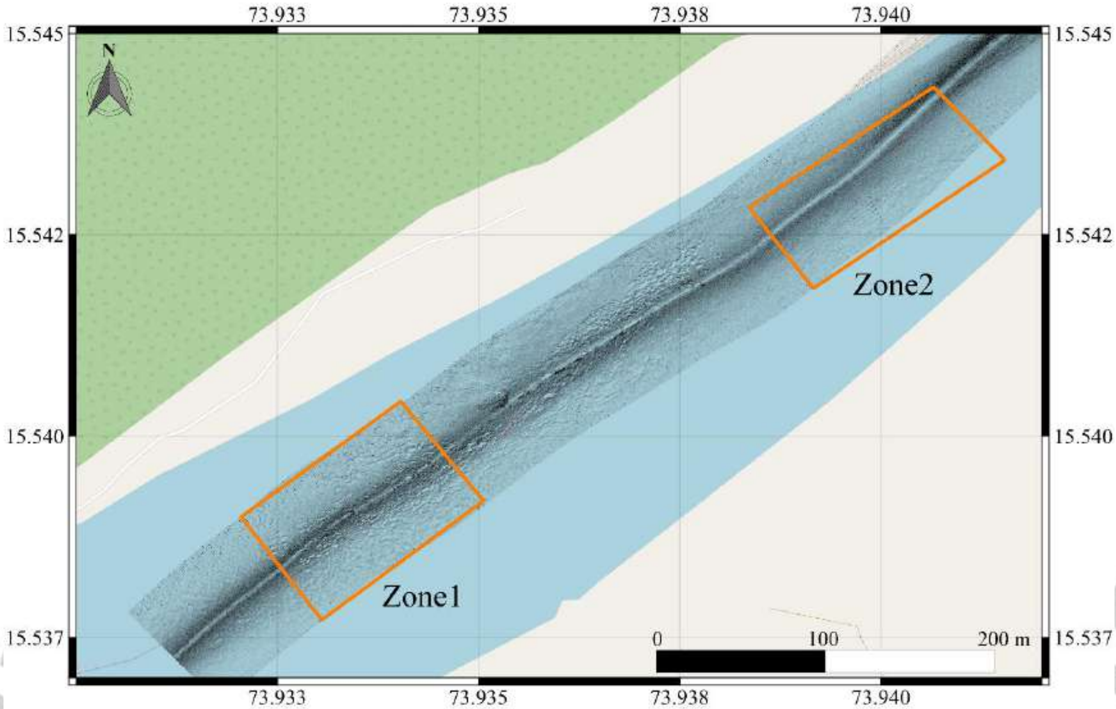

Zone-1 Block Coordinates

S.No.	Longitude	Latitude
1	73.93506	15.53919
2	73.933053	15.53771
3	73.93204	15.53899
4	73.93403	15.54042

Zone-2 Block Coordinates

S.No.	Longitude	Latitude
1	73.94154	15.54343
2	73.93916	15.54183
3	73.93836	15.54284
4	73.94065	15.54434

Zones 3 – 4

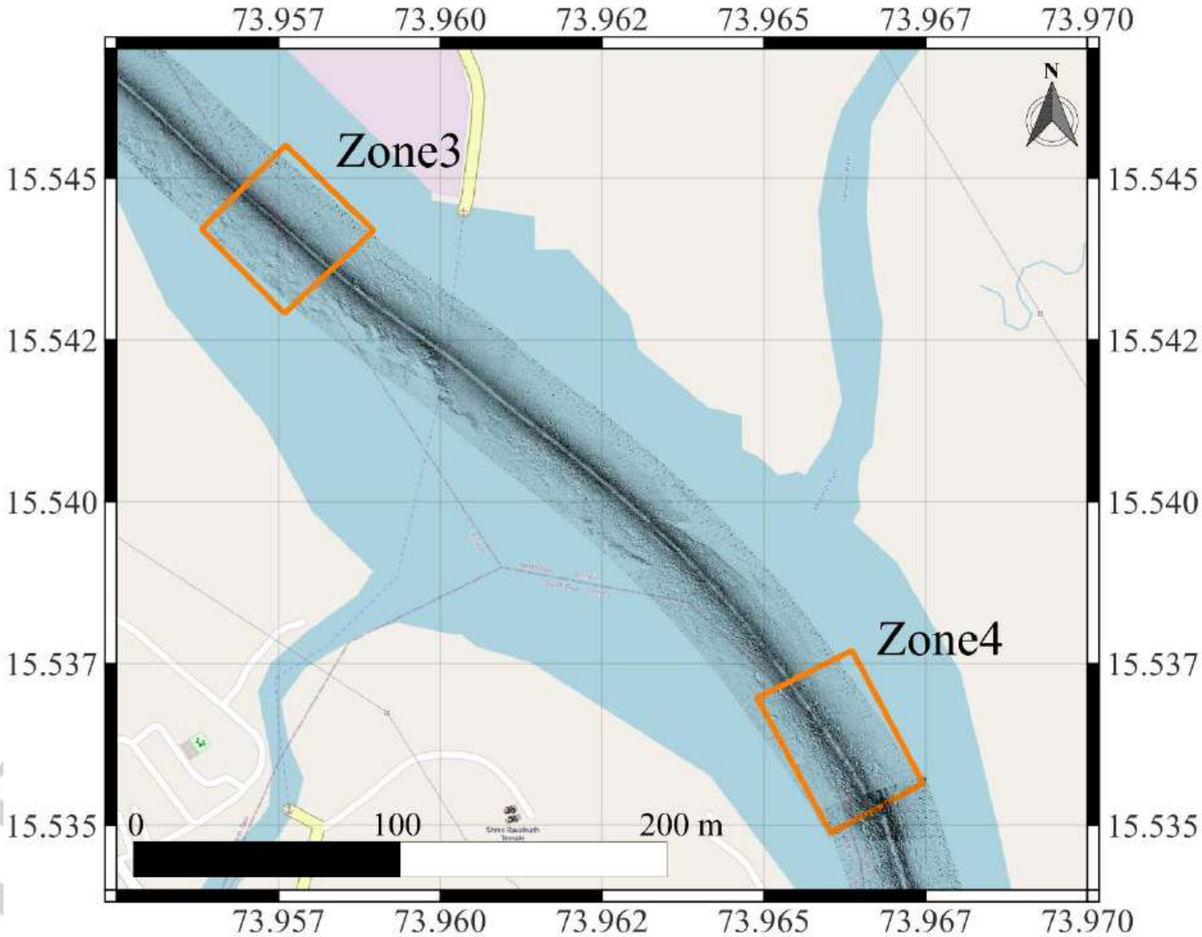

Zone-3 Block Coordinates

S.No.	Longitude	Latitude
1	73.95897	15.54419
2	73.95759	15.54291
3	73.95631	15.54421
4	73.95761	15.54551

Zone-4 Block Coordinates

S.No.	Longitude	Latitude
1	73.96746	15.53564
2	73.96603	15.53487
3	73.96489	15.53696
4	73.96636	15.53770

Zones 5 – 6

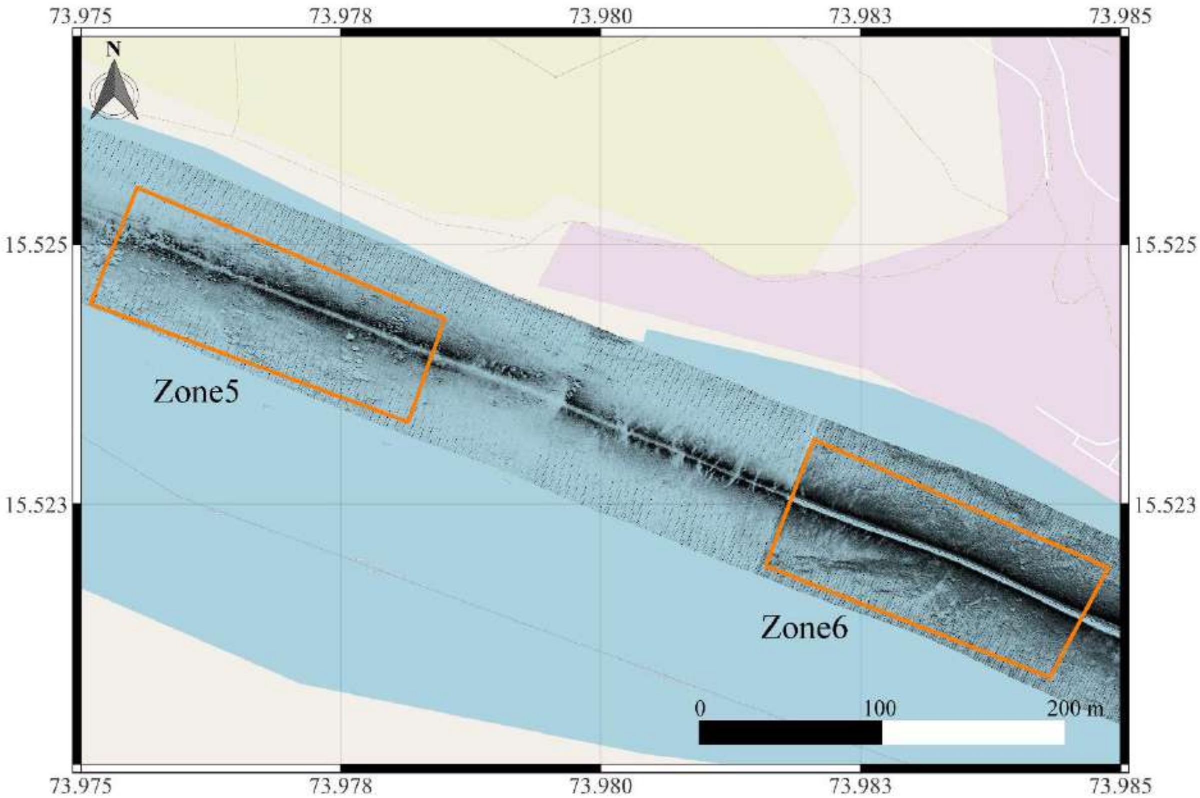

Zone-5 Block Coordinates

S.No.	Longitude	Latitude
1	73.9785	15.52428
2	73.97815	15.52329
3	73.97509	15.52442
4	73.97554	15.52554

Zone-6 Block Coordinates

S.No.	Longitude	Latitude
1	73.98488	15.52188
2	73.98432	15.52083
3	73.98158	15.52190
4	73.98205	15.52312

Zones 7 – 8

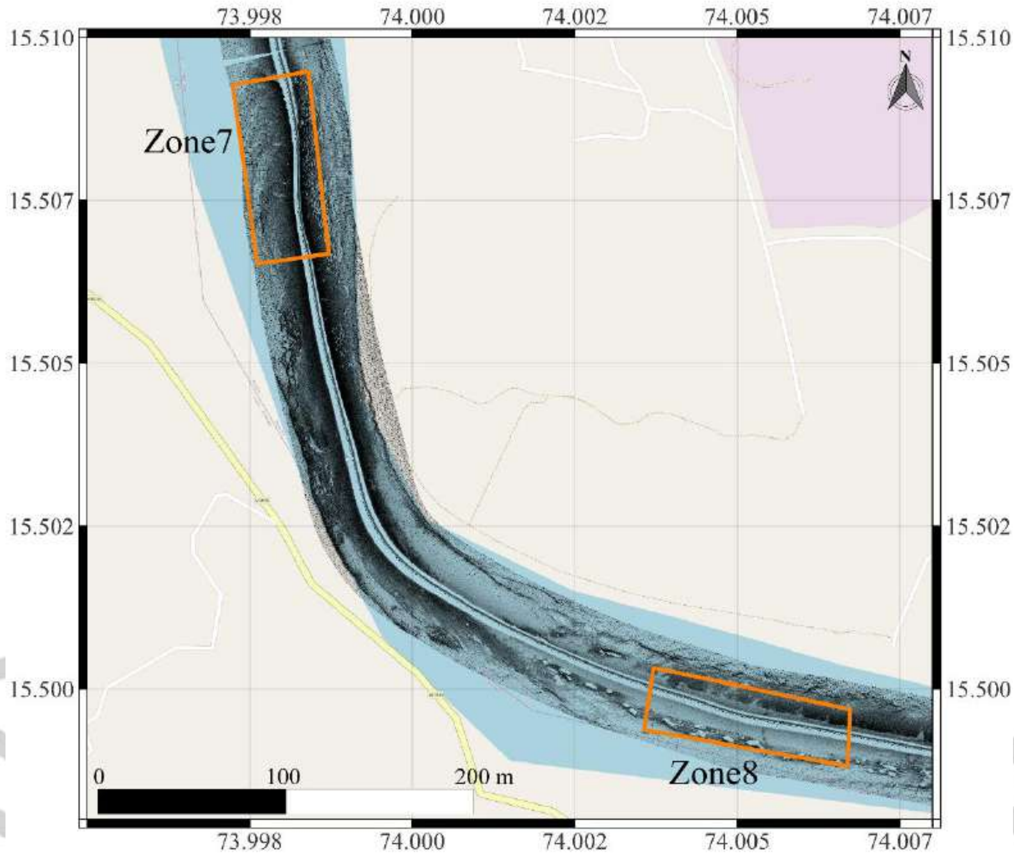

Zone-7 Block Coordinates

S.No.	Longitude	Latitude
1	73.99872	15.50668
2	73.99761	15.50653
3	73.99724	15.50927
4	73.9984	15.50948

Zone-8 Block Coordinates

S.No.	Longitude	Latitude
1	74.00673	15.49968
2	74.00669	15.49881
3	74.00356	15.49937
4	74.00370	15.50032

Zones 9 – 10

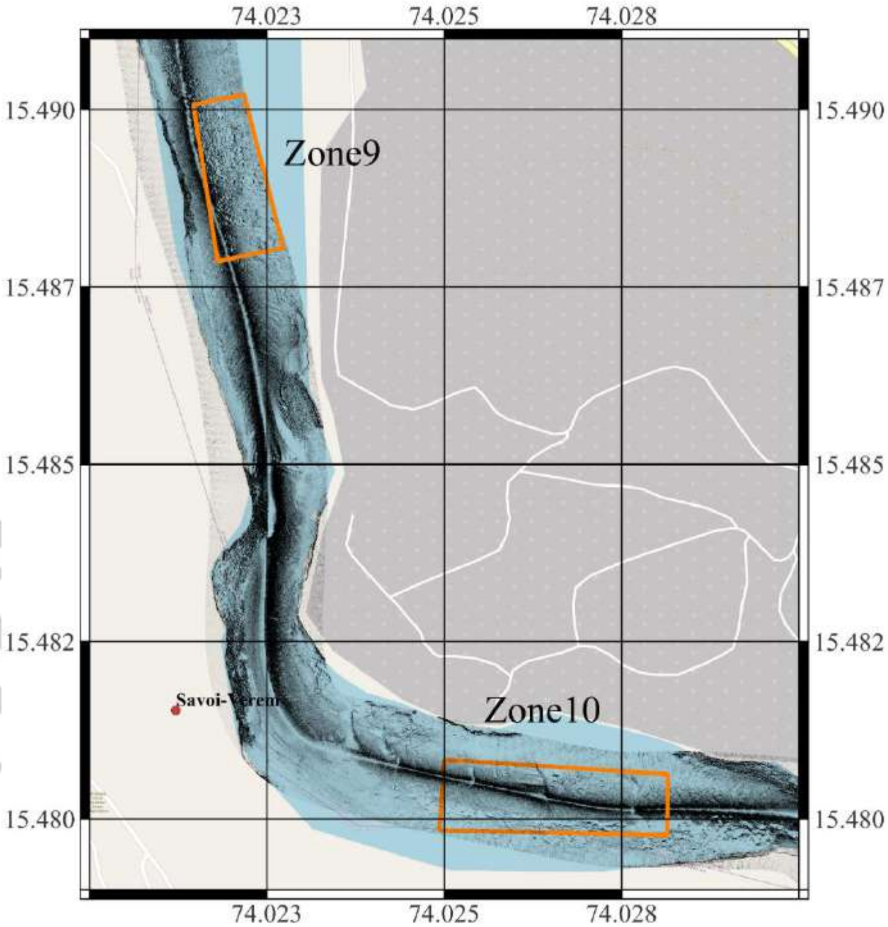

Zone-9 Block Coordinates

S.No.	Longitude	Latitude
1	74.02274	15.48805
2	74.02181	15.48786
3	74.02146	15.49007
4	74.02218	15.49022

Zone-10 Block Coordinates

S.No.	Longitude	Latitude
1	74.02815	15.48062
2	74.02814	15.47977
3	74.02492	15.47983
4	74.02500	15.48083

Identified Sand Mining Zones with quantity

S. No.	Zones	Area (ha)	Volume (Cubic m)	Weight (Tons)
1	Zone1	4.7	52919	84376
2	Zone2	4.2	47290	75399
3	Zone3	4.1	38224	61158
4	Zone4	4.55	44599	71359
5	Zone5	4.3	76043	121669
6	Zone6	4.45	78696	125914
7	Zone7	3.79	90901	145442
8	Zone8	3.1	47485	75976
9	Zone9	2.2	40544	64870
10	Zone10	3.5	71437	114299